

Revealing Language Model Trajectories via Kullback-Leibler Divergence

Ryo Kishino¹ Yusuke Takase¹ Momose Oyama^{1,2}
Hiroaki Yamagiwa¹ Hidetoshi Shimodaira^{1,2}
¹Kyoto University ²RIKEN
kishino.ryo.32s@st.kyoto-u.ac.jp,
{y.takase, oyama.momose}@sys.i.kyoto-u.ac.jp,
{h.yamagiwa, shimo}@i.kyoto-u.ac.jp

Abstract

A recently proposed method enables efficient estimation of the KL divergence between language models, including models with different architectures, by assigning coordinates based on log-likelihood vectors. To better understand the behavior of this metric, we systematically evaluate KL divergence across a wide range of conditions using publicly available language models. Our analysis covers comparisons between pretraining checkpoints, fine-tuned and base models, and layers via the logit lens. We find that trajectories of language models, as measured by KL divergence, exhibit a spiral structure during pretraining and thread-like progressions across layers. Furthermore, we show that, in terms of diffusion exponents, model trajectories in the log-likelihood space are more constrained than those in weight space.

1 Introduction

The growing diversity of language models has created a need to quantify their differences systematically. Treating them as probability distributions over text, the Kullback-Leibler (KL) divergence serves as a natural comparison metric. Oyama et al. (2025) proposed using log-likelihood vectors on a fixed text set to assign model coordinates in a Euclidean space. In this space, the squared distance between models approximates their KL divergence, making model comparison a geometric problem.

However, their analysis did not cover the typical KL divergence values. As an early report on model analysis leveraging log-likelihood vectors, we use publicly available models to measure the KL divergence between checkpoints saved during pretraining (Section 3), fine-tuned and base models (Section 4), and different layers (Section 5) as shown in Table 1.

Furthermore, we analyze the trajectories of language models throughout training and across layers, yielding several notable observations. As shown

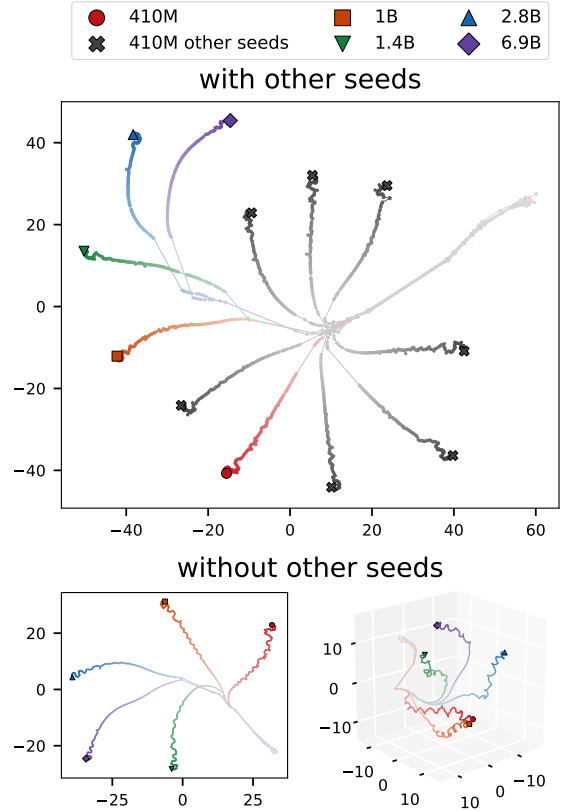


Figure 1: Visualization of the training trajectories of Pythia models using t-SNE applied to log-likelihood vectors. Each point represents a model checkpoint, with lighter colors indicating earlier steps. The thickness of the connecting lines reflects the magnitude of KL divergence between checkpoints. The top panel shows trajectories for five model sizes and multiple random seeds. The bottom panel shows only the five sizes, with both 2D and 3D t-SNE visualizations for clarity. See Section 3 for details.

in Fig. 1, portions of the pretraining trajectories exhibit a spiral structure. Moreover, from the perspective of anomalous diffusion, model dynamics in the log-likelihood space become increasingly constrained during the later steps of training, compared to those in weight space.

	between checkpoints			between seeds	between model sizes			
	10k→11k	50k→51k	100k→101k	avg.	1B	1.4B	2.8B	6.9B
410M	0.069 (±0.0011)	0.053 (±0.0010)	0.023 (±0.00042)	0.11 (± 0.0024)	0.28 (±0.010)	0.52 (±0.018)	1.0 (±0.036)	1.7 (±0.060)

(a) KL divergence for Pythia 410M, measured between checkpoints saved during pretraining, different random seeds, and different model sizes. For the inter-size comparison, the final checkpoints were used. See Section 3 for details.

Type (#pair)	Pair	Median	Mean	SD
mistral (25)	fine-tuning	0.32	0.37	0.32
	random	0.79	0.74	0.39
llama-3 (20)	fine-tuning	0.20	0.67	0.80
	random	0.66	0.87	0.66
all (66)	fine-tuning	0.40	1.5	3.6
	random	2.1	5.0	9.5

(b) Summary statistics (median, mean, SD) of KL divergence between fine-tuned and base models, and between random model pairs. See Section 4 for details.

Model	1→2	16→17	31→32
Llama-2-7b-hf	0.61 (± 0.013)	1.6 (± 0.063)	1.3 (± 0.10)
	4.0 (± 0.075)	22 (± 0.78)	1.7 (± 0.037)
Meta-Llama-3-8B	2.4 (± 0.10)	5.7 (± 0.12)	8.6 (± 0.54)

(c) KL divergence between adjacent layers within models, measured using the logit lens. See Section 5 for details.

Table 1: KL divergence in bits per byte between language models under various conditions. Values in parentheses represent standard errors. See Appendix C for the formula used to compute the standard errors.

2 Review: Model Map

Log-likelihood vector. The probability that a language model p generates a text (i.e., a sequence of tokens) $x = (y_0, \dots, y_M)$ is given by $p(x) = \prod_{m=1}^M p(y_m | y_0, \dots, y_{m-1})$. Oyama et al. (2025) defined the log-likelihood vector of a language model p over a predefined text set $\{x_1, \dots, x_N\}$ as

$$\ell = (\log p(x_1), \dots, \log p(x_N))^T \in \mathbb{R}^N,$$

and showed that it serves as a useful feature representation for comparing models and predicting downstream task performance.

KL divergence. Let $\{p_i\}_{i=1}^K$ be a set of language models, and $\mathbf{L} = (\ell_1, \dots, \ell_K)^T \in \mathbb{R}^{K \times N}$ be the matrix formed by stacking the log-likelihood vectors ℓ_i of each model. Define $\mathbf{Q} = (\mathbf{q}_1, \dots, \mathbf{q}_K)^T$ as the matrix obtained by double-centering¹ \mathbf{L} . Then, the KL divergence between two models p_i and p_j can be approximated as

$$2\text{KL}(p_i, p_j) \approx \|\mathbf{q}_i - \mathbf{q}_j\|^2 / N.$$

In other words, by associating each model p_i with a coordinate $\mathbf{q}_i \in \mathbb{R}^N$, KL divergence is approximated by squared Euclidean distance in this space. This coordinate system is referred to as the model map in Oyama et al. (2025). In particular, we refer to a sequence of models represented as coordinates in the model map as a trajectory.

General experimental settings. For the text set, we use the same 10,000 texts extracted from the

¹Row-wise centering followed by column-wise centering.

Pile (Gao et al., 2020) as in Oyama et al. (2025)². The values of KL divergence are normalized by the average text length, $\bar{B} = 972.3188$ bytes, and are reported in units of bits per byte. In particular, the matrix \mathbf{Q} is divided by $\sqrt{2N\bar{B}\log 2}$ in advance, so that the squared Euclidean distance directly approximates the KL divergence in bits per byte. All visualizations are based on this \mathbf{Q} .

3 Pretraining

In the Pythia suite (Biderman et al., 2023), the checkpoints saved during pretraining are publicly available for each model size. Additionally, van der Wal et al. (2025) released checkpoints for smaller Pythia models trained with different random seeds. In this section, we investigate how a language model’s trajectory evolves during pretraining by analyzing these checkpoints.

Settings. We use checkpoints from the standard Pythia models with sizes 410M, 1B, 1.4B, 2.8B, and 6.9B. In addition, for the 410M model, we supplement our analysis with checkpoints from seven different random seeds. The checkpoints are saved at training steps 0, 1, 2, 4, ..., 512, 1k, 2k, 3k, ..., and 143k. We excluded the 1B checkpoint at step 116k due to anomalous weights, and removed texts with irregular log-likelihood variations across checkpoints. See Appendix D.1 for details.

KL divergence. Table 1a shows the KL divergence for Pythia 410M. The KL divergence between checkpoints saved every 1k steps gradually

²<https://github.com/shimo-lab/modelmap/>

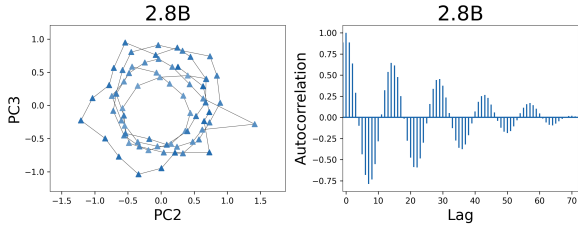


Figure 2: Trajectory of Pythia 2.8B during pretraining, visualized by applying 3D t-SNE, followed by PCA on the later half portion. (Left) PC2 vs. PC3. (Right) Autocorrelation function of PC3.

Model Size	410M	1B	1.4B	2.8B	6.9B
Period (step)	30k	13k	15k	14k	12k

Table 2: Period of the spiral trajectory of Pythia during pretraining. See Appendix D.3 for details.

decreases as training progresses, and after step 10k, it stays within a small range (approximately 0.02 to 0.07 bit/byte), as also shown in the right panel of Fig. 4. Moreover, the values between different random seeds are around 0.1 bit/byte, while those between different sizes range from 0.3 to 2 bit/byte, indicating larger differences. See Appendix D.2 for details.

Trajectory. Fig. 1 shows a simultaneous visualization of the pretraining trajectories of five model sizes using t-SNE (van der Maaten and Hinton, 2008)³, which is not possible with weight-based representations. The trajectories evolve continuously during training⁴. Moreover, the 3D visualization suggests that the trajectories exhibit a spiral structure. As shown in Fig. 2, applying PCA to the later portion of the trajectory obtained via t-SNE reveals a circular pattern. The autocorrelation function of PC3 exhibits periodicity. The estimated periods of the spiral trajectories are shown in Table 2. Similar phenomena in weight trajectories have been studied previously (Cohen et al., 2021; Netay, 2024) described in detail in Appendix A. In addition, refer to Appendix D.4 for a trajectory visualization using PCA.

Comparison with weights. Differences between models with the same architecture can be measured by the distance between their weights. Let \mathbf{W}_t be the weights of a neural network at step t . According to Kunin et al. (2024), after model performance has

³We used the scikit-learn implementation with the default perplexity value of 30.

⁴The apparent jumps in the 2D trajectories of the 2.8B and 6.9B models are artifacts of t-SNE, which tends to separate overlapping points. These trajectories appear continuous in 3D t-SNE visualizations.

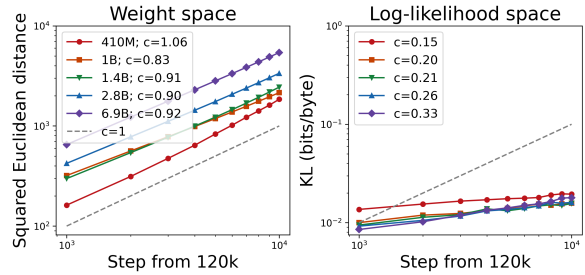


Figure 3: Temporal evolution of the squared Euclidean distance in the weights and log-likelihood vectors from step 120k to step 130k for Pythia. The diffusion exponent c is estimated using the least squares method.

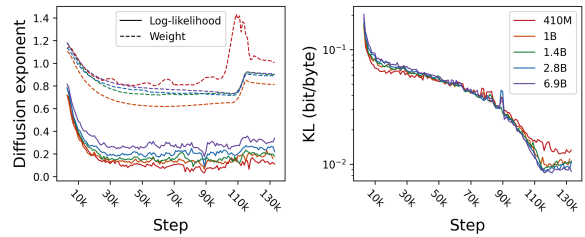


Figure 4: (Left) Diffusion exponent c as a function of the starting point t_0 . (Right) KL divergence between consecutive checkpoints of Pythia (corresponding to Table 1a). See Appendix D.5 for details.

converged, the weights diffuse following a power law with exponent c^5 . That is, with respect to an initial step t_0 , the relationship $\|\mathbf{W}_t - \mathbf{W}_{t_0}\|^2 \propto |t - t_0|^c$ holds, where c may differ from 1.

To verify this, we measured the evolution of the squared Euclidean distance in both the weights \mathbf{W} and the log-likelihood vectors \mathbf{q} , over steps 120k to 130k of Pythia. As shown in Fig. 3, both \mathbf{W} and \mathbf{q} follow a power-law relationship with exponents c_w and c_q respectively. The weights \mathbf{W} exhibit Brownian-like diffusion ($c_w \approx 1$), whereas the diffusion of \mathbf{q} is substantially suppressed ($c_q \approx 0.2$). In addition, Fig. 4 illustrates how the exponents c_w and c_q vary with the starting step. Notably, c_q remains consistently smaller than c_w throughout. Both c_w and c_q tend to decrease as training progresses. However, around step 120k, when the KL divergence between successive checkpoints stabilizes, c_w increases, while c_q shows no significant change. As discussed in Appendix B, the difference in dynamics between these two spaces could be explained by the flat minima hypothesis (Keskar et al., 2017) and by constraints imposed by the loss

⁵Brownian motion corresponds to $c = 1$, while anomalous diffusion is defined as $c \neq 1$. Specifically, $c > 1$ means superdiffusion, and $c < 1$ means subdiffusion. If the evolution is fractional Brownian motion (Mandelbrot and Van Ness, 1968), the Hurst exponent corresponds to $H = c/2$.

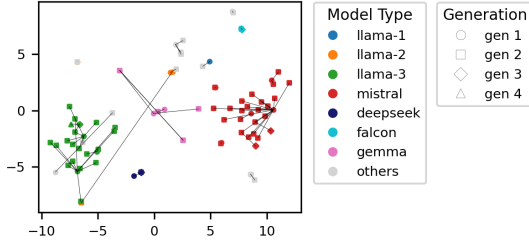


Figure 5: Map showing base models and their fine-tuned variants. Lines represent parent-child relationships between models. Colors indicate model types as defined in Oyama et al. (2025). Generation refers to the depth from the root model within each lineage.

function on the log-likelihood space.

4 Fine-tuning

The introduction of efficient fine-tuning methods (Hu et al., 2022; Rafailov et al., 2023) has led to the development of a large number of fine-tuned models. In this section, we investigate the KL divergence between fine-tuned and base models.

Settings. Out of the 1,018 language models analyzed in Oyama et al. (2025), we use 66 pairs of fine-tuned and base models (87 models in total; Fig. 5). The parent-child relationships are identified using Hugging Face Hub API. See Appendix E for details.

KL divergence. Table 1b shows the statistics on the KL divergence between fine-tuned and base models, and between randomly selected models. For the cumulative distribution, see Fig. 18 in Appendix E. KL divergence values tend to be slightly smaller for models of type mistral or llama-3. In all cases, the KL divergence between fine-tuned and base models is smaller than that between random pairs, with a median ranging from 0.2 to 0.4 bit/byte.

5 Layer

We investigate model trajectories across layers by treating the network up to each layer as an individual model using the logit lens (nostalgebraist, 2020).

Settings. We use a subset of the 1,018 language models analyzed in Oyama et al. (2025). First, without restricting model types, we select the 50 most downloaded models (Fig. 6). When limiting to specific model types, we use the 10 most downloaded

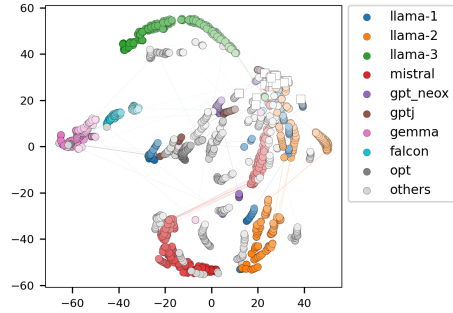


Figure 6: t-SNE visualization of trajectories across layers for 50 models, obtained by applying the logit lens to each layer. Deeper layers are represented with lighter colors, and the final layer is indicated by a white square.

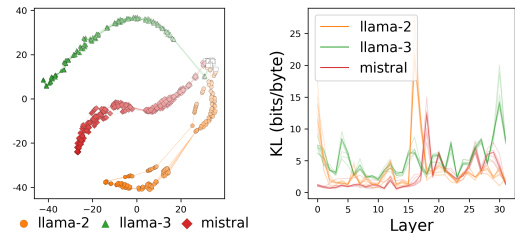


Figure 7: For 10 models per model type: (left) t-SNE visualization of trajectories across layers, where the final layer is indicated by a white square; (right) KL divergence between adjacent layers (corresponding to Table 1c). See Fig. 20 in Appendix F for a 3D plot.

models from each of the llama-2, llama-3, and mistral with 32 layers (30 models in total; Fig. 7). See Appendix F for details on the models used.

KL divergence. The right panel of Fig. 7 and Table 1c show the KL divergence between consecutive layers. Models of the same type exhibit similar trends. For llama-2, Wendler et al. (2024) reported a sharp drop in the entropy of next-token distributions at intermediate layers in a translation task, which corresponds to the peak positions in Fig. 7. The KL divergence between consecutive layers ranges from as low as 1 bit/byte to as high as 10 to 25 bit/byte, indicating substantial variation.

Trajectory. Fig. 6 and the left panel of Fig. 7 illustrate the model trajectories across layers. The trajectories exhibit jumps at KL divergence peaks and tend to align in deeper layers. The trajectories align with increasing mean log-likelihood (Fig. 19, Appendix F).

6 Conclusion

We analyzed KL divergence and trajectories across checkpoints, model pairs, and layers, revealing spiral and aligned structures over training and depth.

Limitations

- The checkpoints for Pythia are available only at 1k-step intervals except for the early stages of training. When checkpoints are saved at shorter intervals, the resulting trajectories can differ from our observation. In particular, the estimation of the diffusion exponent may be affected by errors introduced by the coarse granularity of the 1k-step resolution.
- The KL divergence we measured depends on the text set used. In future work, we plan to investigate how the KL divergence and model trajectories vary when a different text set is used.
- The number of models used is limited in the experiment measuring KL divergence between fine-tuned and base models. This is because some fine-tuned models do not include information about their base models in their model cards obtained by using Hugging Face Hub API.
- In the layer-wise analysis, the logits obtained from shallow layers via the logit lens contain substantial noise. This issue could be addressed by using the tuned lens (Belrose et al., 2023), an improved version of the logit lens. However, the number of publicly available pretrained tuned lenses is currently limited. We believe this limitation can be overcome in the future by training tuned lenses ourselves.
- While we observe structured behaviors such as spiral trajectories and subdiffusion in the log-likelihood space, their underlying causes and implications for learning dynamics have not been quantitatively analyzed and remain open for future investigation.

Acknowledgments

We thank Luis Iván Hernández Ruíz for helpful discussions. This study was partially supported by JSPS KAKENHI 22H05106, 23H03355, JST CREST JPMJCR21N3, JST BOOST JP-MJBS2407.

References

01. AI, Alex Young, Bei Chen, Chao Li, Chengen Huang, Ge Zhang, Guanwei Zhang, Guoyin Wang, Heng Li, Jiangcheng Zhu, Jianqun Chen, Jing Chang,

Kaidong Yu, Peng Liu, Qiang Liu, Shawn Yue, Senbin Yang, Shiming Yang, Wen Xie, and 13 others. 2025. [Yi: Open foundation models by 01.ai](#). *Preprint*, arXiv:2403.04652.

AI@Meta. 2024. [Llama 3 model card](#).

Joshua Ainslie, James Lee-Thorp, Michiel de Jong, Yury Zemlyanskiy, Federico Lebrón, and Sumit Sanghai. 2023. [Gqa: Training generalized multi-query transformer models from multi-head checkpoints](#). *Preprint*, arXiv:2305.13245.

AI@Waktaverse. 2024. [Waktaverse llama 3 model card](#).

Ebtesam Almazrouei, Hamza Alobeidli, Abdulaziz Alshamsi, Alessandro Cappelli, Ruxandra Cojocaru, Merouane Debbah, Etienne Goffinet, Daniel Hestlow, Julien Launay, Quentin Malartic, Badreddine Noune, Baptiste Pannier, and Guilherme Penedo. 2023. [Falcon-40B: an open large language model with state-of-the-art performance](#).

Alex Andonian, Quentin Anthony, Stella Biderman, Sid Black, Preetham Gali, Leo Gao, Eric Hallahan, Josh Levy-Kramer, Connor Leahy, Lucas Nestler, Kip Parker, Michael Pieler, Shivanshu Purohit, Tri Songz, Wang Phil, and Samuel Weinbach. 2021. [GPT-NeoX: Large scale autoregressive language modeling in PyTorch](#).

Sanjeev Arora, Zhiyuan Li, and Abhishek Panigrahi. 2022. [Understanding gradient descent on the edge of stability in deep learning](#). In *International Conference on Machine Learning, ICML 2022, 17-23 July 2022, Baltimore, Maryland, USA*, volume 162 of *Proceedings of Machine Learning Research*, pages 948–1024. PMLR.

Jacob Austin, Augustus Odena, Maxwell Nye, Maarten Bosma, Henryk Michalewski, David Dohan, Ellen Jiang, Carrie Cai, Michael Terry, Quoc Le, and Charles Sutton. 2021. [Program synthesis with large language models](#). *Preprint*, arXiv:2108.07732.

Jinze Bai, Shuai Bai, Yunfei Chu, Zeyu Cui, Kai Dang, Xiaodong Deng, Yang Fan, Wenbin Ge, Yu Han, Fei Huang, Binyuan Hui, Luo Ji, Mei Li, Junyang Lin, Runji Lin, Dayiheng Liu, Gao Liu, Chengqiang Lu, Keming Lu, and 29 others. 2023. [Qwen technical report](#). *Preprint*, arXiv:2309.16609.

Pierpaolo Basile, Elio Musacchio, Marco Polignano, Lucia Siciliani, Giuseppe Fiameni, and Giovanni Semeraro. 2023. [Llamantino: Llama 2 models for effective text generation in italian language](#). *Preprint*, arXiv:2312.09993.

Mohammad Bavarian, Heewoo Jun, Nikolas Tezak, John Schulman, Christine McLeavey, Jerry Tworek, and Mark Chen. 2022. [Efficient training of language models to fill in the middle](#). *Preprint*, arXiv:2207.14255.

- Nora Belrose, Zach Furman, Logan Smith, Danny Halawi, Igor Ostrovsky, Lev McKinney, Stella Biderman, and Jacob Steinhardt. 2023. [Eliciting latent predictions from transformers with the tuned lens](#). *Preprint*, arXiv:2303.08112.
- Iz Beltagy, Matthew E. Peters, and Arman Cohan. 2020. [Longformer: The long-document transformer](#). *Preprint*, arXiv:2004.05150.
- Stella Biderman, Kieran Bicheno, and Leo Gao. 2022. [Datasheet for the pile](#). *Preprint*, arXiv:2201.07311.
- Stella Biderman, Hailey Schoelkopf, Quentin Anthony, Herbie Bradley, Kyle O’Brien, Eric Hallahan, Mohammad Aflah Khan, Shivanshu Purohit, USVSN Sai Prashanth, Edward Raff, Aviya Skowron, Lintang Sutawika, and Oskar van der Wal. 2023. [Pythia: A suite for analyzing large language models across training and scaling](#). *Preprint*, arXiv:2304.01373.
- Yonatan Bisk, Rowan Zellers, Ronan Le Bras, Jianfeng Gao, and Yejin Choi. 2019. [Piqa: Reasoning about physical commonsense in natural language](#). *Preprint*, arXiv:1911.11641.
- Sid Black, Gao Leo, Phil Wang, Connor Leahy, and Stella Biderman. 2021. [GPT-Neo: Large Scale Autoregressive Language Modeling with Mesh-Tensorflow](#). If you use this software, please cite it using these metadata.
- Tom B. Brown, Benjamin Mann, Nick Ryder, Melanie Subbiah, Jared Kaplan, Prafulla Dhariwal, Arvind Neelakantan, Pranav Shyam, Girish Sastry, Amanda Askell, Sandhini Agarwal, Ariel Herbert-Voss, Gretchen Krueger, Tom Henighan, Rewon Child, Aditya Ramesh, Daniel M. Ziegler, Jeffrey Wu, Clemens Winter, and 12 others. 2020. [Language models are few-shot learners](#). *Preprint*, arXiv:2005.14165.
- Mark Chen, Jerry Tworek, Heewoo Jun, Qiming Yuan, Henrique Ponde de Oliveira Pinto, Jared Kaplan, Harri Edwards, Yuri Burda, Nicholas Joseph, Greg Brockman, Alex Ray, Raul Puri, Gretchen Krueger, Michael Petrov, Heidy Khlaaf, Girish Sastry, Pamela Mishkin, Brooke Chan, Scott Gray, and 39 others. 2021. [Evaluating large language models trained on code](#). *Preprint*, arXiv:2107.03374.
- François Chollet. 2019. [On the measure of intelligence](#). *Preprint*, arXiv:1911.01547.
- Christopher Clark, Kenton Lee, Ming-Wei Chang, Tom Kwiatkowski, Michael Collins, and Kristina Toutanova. 2019. [Boolq: Exploring the surprising difficulty of natural yes/no questions](#). *Preprint*, arXiv:1905.10044.
- Karl Cobbe, Vineet Kosaraju, Mohammad Bavarian, Mark Chen, Heewoo Jun, Lukasz Kaiser, Matthias Plappert, Jerry Tworek, Jacob Hilton, Reiichiro Nakano, Christopher Hesse, and John Schulman. 2021. [Training verifiers to solve math word problems](#). *Preprint*, arXiv:2110.14168.
- Jeremy Cohen, Simran Kaur, Yuanzhi Li, J. Zico Kolter, and Ameet Talwalkar. 2021. [Gradient descent on neural networks typically occurs at the edge of stability](#). In *9th International Conference on Learning Representations, ICLR 2021, Virtual Event, Austria, May 3-7, 2021*. OpenReview.net.
- Ganqu Cui, Lifan Yuan, Ning Ding, Guanming Yao, Bingxiang He, Wei Zhu, Yuan Ni, Guotong Xie, Ruobing Xie, Yankai Lin, Zhiyuan Liu, and Maosong Sun. 2024. [Ultrafeedback: Boosting language models with scaled ai feedback](#). *Preprint*, arXiv:2310.01377.
- Tri Dao, Daniel Y. Fu, Stefano Ermon, Atri Rudra, and Christopher Ré. 2022. [Flashattention: Fast and memory-efficient exact attention with io-awareness](#). *Preprint*, arXiv:2205.14135.
- Tim Dettmers, Artidoro Pagnoni, Ari Holtzman, and Luke Zettlemoyer. 2023. [Qlora: Efficient finetuning of quantized llms](#). *Preprint*, arXiv:2305.14314.
- Peter Devine. 2024. [Tagengo: A multilingual chat dataset](#). *Preprint*, arXiv:2405.12612.
- Jwala Dhamala, Tony Sun, Varun Kumar, Satyapriya Krishna, Yada Pruksachatkun, Kai-Wei Chang, and Rahul Gupta. 2021. [Bold: Dataset and metrics for measuring biases in open-ended language generation](#). *Preprint*, arXiv:2101.11718.
- Ning Ding, Yulin Chen, Bokai Xu, Yujia Qin, Zhi Zheng, Shengding Hu, Zhiyuan Liu, Maosong Sun, and Bowen Zhou. 2023. [Enhancing chat language models by scaling high-quality instructional conversations](#). *Preprint*, arXiv:2305.14233.
- Victor Gallego. 2024. [Configurable safety tuning of language models with synthetic preference data](#). *Preprint*, arXiv:2404.00495.
- Leo Gao, Stella Biderman, Sid Black, Laurence Golding, Travis Hoppe, Charles Foster, Jason Phang, Horace He, Anish Thite, Noa Nabeshima, Shawn Presser, and Connor Leahy. 2020. [The pile: An 800gb dataset of diverse text for language modeling](#). *Preprint*, arXiv:2101.00027.
- Samuel Gehman, Suchin Gururangan, Maarten Sap, Yejin Choi, and Noah A. Smith. 2020. [Realtocixityprompts: Evaluating neural toxic degeneration in language models](#). *Preprint*, arXiv:2009.11462.
- Gemini Team, Rohan Anil, Sebastian Borgeaud, Jean-Baptiste Alayrac, Jiahui Yu, Radu Soricut, Johan Schalkwyk, Andrew M. Dai, Anja Hauth, Katie Millican, David Silver, Melvin Johnson, Ioannis Antonoglou, Julian Schrittwieser, Amelia Glaese, Jilin Chen, Emily Pitler, Timothy Lillicrap, Angeliki Lazaridou, and 1331 others. 2024. [Gemini: A family of highly capable multimodal models](#). *Preprint*, arXiv:2312.11805.
- Xinyang Geng and Hao Liu. 2023. [Openllama: An open reproduction of llama](#).

- Thomas Hartvigsen, Saadia Gabriel, Hamid Palangi, Maarten Sap, Dipankar Ray, and Ece Kamar. 2022. [Toxigen: A large-scale machine-generated dataset for adversarial and implicit hate speech detection](#). *Preprint*, arXiv:2203.09509.
- Dan Hendrycks, Collin Burns, Steven Basart, Andy Zou, Mantas Mazeika, Dawn Song, and Jacob Steinhardt. 2021. [Measuring massive multitask language understanding](#). *Preprint*, arXiv:2009.03300.
- Alex Henry, Prudhvi Raj Dachapally, Shubham Pawar, and Yuxuan Chen. 2020. [Query-key normalization for transformers](#). *Preprint*, arXiv:2010.04245.
- Jiwoo Hong, Noah Lee, and James Thorne. 2024. [Orpo: Monolithic preference optimization without reference model](#). *Preprint*, arXiv:2403.07691.
- Edward J. Hu, Yelong Shen, Phillip Wallis, Zeyuan Allen-Zhu, Yuanzhi Li, Shean Wang, Lu Wang, and Weizhu Chen. 2022. [Lora: Low-rank adaptation of large language models](#). In *The Tenth International Conference on Learning Representations, ICLR 2022, Virtual Event, April 25-29, 2022*. OpenReview.net.
- "interstellarninja", "Teknium", "theemozilla", "karan4d", and "huemin_art". 2024. [Hermes-2-pro-mistral-7b](#).
- Albert Q. Jiang, Alexandre Sablayrolles, Arthur Mensch, Chris Bamford, Devendra Singh Chaplot, Diego de las Casas, Florian Bressand, Gianna Lengyel, Guillaume Lample, Lucile Saulnier, L  lio Renard Lavaud, Marie-Anne Lachaux, Pierre Stock, Teven Le Scao, Thibaut Lavril, Thomas Wang, Timoth  e Lacroix, and William El Sayed. 2023. [Mistral 7b](#). *Preprint*, arXiv:2310.06825.
- Mandar Joshi, Eunsol Choi, Daniel S. Weld, and Luke Zettlemoyer. 2017. [Triviaqa: A large scale distantly supervised challenge dataset for reading comprehension](#). *Preprint*, arXiv:1705.03551.
- Nitish Shirish Keskar, Dheevatsa Mudigere, Jorge Nocedal, Mikhail Smelyanskiy, and Ping Tak Peter Tang. 2017. [On large-batch training for deep learning: Generalization gap and sharp minima](#). In *International Conference on Learning Representations*.
- Dahyun Kim, Yungi Kim, Wonho Song, Hyeonwoo Kim, Yunsu Kim, Sanghoon Kim, and Chanjun Park. 2024a. [sdpo: Don't use your data all at once](#). *Preprint*, arXiv:2403.19270.
- Dahyun Kim, Chanjun Park, Sanghoon Kim, Wonsung Lee, Wonho Song, Yunsu Kim, Hyeonwoo Kim, Yungi Kim, Hyeonju Lee, Jihoo Kim, Changbae Ahn, Seonghoon Yang, Sukyung Lee, Hyunbyung Park, Gyoungjin Gim, Mikyoung Cha, Hwalsuk Lee, and Sunghun Kim. 2024b. [Solar 10.7b: Scaling large language models with simple yet effective depth up-scaling](#). *Preprint*, arXiv:2312.15166.
- Daniel Kunin, Javier Sagastuy-Bre  a, Lauren E. Gillespie, Eshed Margalit, Hidenori Tanaka, Surya Ganguli, and Daniel L. K. Yamins. 2024. [The limiting dynamics of SGD: modified loss, phase-space oscillations, and anomalous diffusion](#). *Neural Comput.*, 36(1):151–174.
- Alexandre Lacoste, Alexandra Luccioni, Victor Schmidt, and Thomas Dandres. 2019. [Quantifying the carbon emissions of machine learning](#). *Preprint*, arXiv:1910.09700.
- Yuanzhi Li, S  bastien Bubeck, Ronen Eldan, Allie Del Giorno, Suriya Gunasekar, and Yin Tat Lee. 2023. [Textbooks are all you need ii: phi-1.5 technical report](#). *Preprint*, arXiv:2309.05463.
- Stephanie Lin, Jacob Hilton, and Owain Evans. 2022. [Truthfulqa: Measuring how models mimic human falsehoods](#). *Preprint*, arXiv:2109.07958.
- Nelson F. Liu, Kevin Lin, John Hewitt, Ashwin Paranjape, Michele Bevilacqua, Fabio Petroni, and Percy Liang. 2023. [Lost in the middle: How language models use long contexts](#). *Preprint*, arXiv:2307.03172.
- Anton Lozhkov, Raymond Li, Loubna Ben Allal, Federico Cassano, Joel Lamy-Poirier, Nouamane Tazi, Ao Tang, Dmytro Pykhtar, Jiawei Liu, Yuxiang Wei, Tianyang Liu, Max Tian, Denis Kocetkov, Arthur Zucker, Younes Belkada, Zijian Wang, Qian Liu, Dmitry Abulkhanov, Indraneil Paul, and 47 others. 2024. [Starcoder 2 and the stack v2: The next generation](#). *Preprint*, arXiv:2402.19173.
- Benoit B Mandelbrot and John W Van Ness. 1968. Fractional brownian motions, fractional noises and applications. *SIAM review*, 10(4):422–437.
- Todor Mihaylov, Peter Clark, Tushar Khot, and Ashish Sabharwal. 2018. [Can a suit of armor conduct electricity? a new dataset for open book question answering](#). *Preprint*, arXiv:1809.02789.
- Arindam Mitra, Luciano Del Corro, Shweti Mahajan, Andres Coda, Clarisse Simoes, Sahaj Agarwal, Xuxi Chen, Anastasia Razdaibiedina, Erik Jones, Kriti Agarwal, Hamid Palangi, Guoqing Zheng, Corby Rosset, Hamed Khanpour, and Ahmed Awadallah. 2023. [Orca 2: Teaching small language models how to reason](#). *Preprint*, arXiv:2311.11045.
- Koh Mitsuda, Xinqi Chen, Toshiaki Wakatsuki, and Kei Sawada. 2024. [rinna/llama-3-youko-8b](#).
- MosaicML NLP Team. 2023. [Introducing mpt-7b: A new standard for open-source, commercially usable llms](#). Accessed: 2023-03-28.
- Niklas Muennighoff, Hongjin Su, Liang Wang, Nan Yang, Furu Wei, Tao Yu, Amanpreet Singh, and Douwe Kiela. 2025. [Generative representational instruction tuning](#). *Preprint*, arXiv:2402.09906.

- Subhabrata Mukherjee, Arindam Mitra, Ganesh Jawahar, Sahaj Agarwal, Hamid Palangi, and Ahmed Awadallah. 2023. [Orca: Progressive learning from complex explanation traces of gpt-4](#). *Preprint*, arXiv:2306.02707.
- Igor V. Netay. 2024. [Geometrical structures of digital fluctuations in parameter space of neural networks trained with adaptive momentum optimization](#). *Preprint*, arXiv:2408.12273.
- Nexusflow.ai team. 2023. [Nexusraven-v2: Surpassing gpt-4 for zero-shot function calling](#).
- Harsha Nori, Nicholas King, Scott Mayer McKinney, Dean Carignan, and Eric Horvitz. 2023. [Capabilities of gpt-4 on medical challenge problems](#). *Preprint*, arXiv:2303.13375.
- nostalgebraist. 2020. [interpreting gpt: the logit lens](#). *LessWrong*.
- OpenAI, Josh Achiam, Steven Adler, Sandhini Agarwal, Lama Ahmad, Ilge Akkaya, Florencia Leoni Aleman, Diogo Almeida, Janko Altenschmidt, Sam Altman, Shyamal Anadkat, Red Avila, Igor Babuschkin, Suchir Balaji, Valerie Balcom, Paul Baltescu, Haiming Bao, Mohammad Bavarian, Jeff Belgum, and 262 others. 2024. [Gpt-4 technical report](#). *Preprint*, arXiv:2303.08774.
- Momose Oyama, Hiroaki Yamagiwa, Yusuke Takase, and Hidetoshi Shimodaira. 2025. [Mapping 1,000+ language models via the log-likelihood vector](#). *Preprint*, arXiv:2502.16173.
- Ankit Pal and Malaikannan Sankarasubbu. 2024a. [Gemini goes to med school: Exploring the capabilities of multimodal large language models on medical challenge problems & hallucinations](#). *Preprint*, arXiv:2402.07023.
- Ankit Pal and Malaikannan Sankarasubbu. 2024b. [Openbiollms: Advancing open-source large language models for healthcare and life sciences](#).
- Arka Pal, Deep Karkhanis, Samuel Dooley, Manley Roberts, Siddartha Naidu, and Colin White. 2024. [Smaug: Fixing failure modes of preference optimization with dpo-positive](#). *Preprint*, arXiv:2402.13228.
- Alicia Parrish, Angelica Chen, Nikita Nangia, Vishakh Padmakumar, Jason Phang, Jana Thompson, Phu Mon Htut, and Samuel R. Bowman. 2022. [Bbq: A hand-built bias benchmark for question answering](#). *Preprint*, arXiv:2110.08193.
- Guilherme Penedo, Quentin Malartic, Daniel Hesslow, Ruxandra Cojocaru, Alessandro Cappelli, Hamza Alobeidli, Baptiste Pannier, Ebtesam Almazrouei, and Julien Launay. 2023. [The refinedweb dataset for falcon llm: Outperforming curated corpora with web data, and web data only](#). *Preprint*, arXiv:2306.01116.
- Marco Polignano, Pierpaolo Basile, and Giovanni Semeraro. 2024. [Advanced natural-based interaction for the italian language: Llamantino-3-anita](#). *Preprint*, arXiv:2405.07101.
- Ofir Press, Noah A. Smith, and Mike Lewis. 2022. [Train short, test long: Attention with linear biases enables input length extrapolation](#). *Preprint*, arXiv:2108.12409.
- Rafael Rafailov, Archit Sharma, Eric Mitchell, Stefano Ermon, Christopher D. Manning, and Chelsea Finn. 2024. [Direct preference optimization: Your language model is secretly a reward model](#). *Preprint*, arXiv:2305.18290.
- Rafael Rafailov, Archit Sharma, Eric Mitchell, Christopher D. Manning, Stefano Ermon, and Chelsea Finn. 2023. [Direct preference optimization: Your language model is secretly a reward model](#). In *Advances in Neural Information Processing Systems 36: Annual Conference on Neural Information Processing Systems 2023, NeurIPS 2023, New Orleans, LA, USA, December 10 - 16, 2023*.
- Baptiste Rozière, Jonas Gehring, Fabian Gloeckle, Sten Sootla, Itai Gat, Xiaoqing Ellen Tan, Yossi Adi, Jingyu Liu, Romain Sauvestre, Tal Remez, Jérémy Rapin, Artyom Kozhevnikov, Ivan Evtimov, Joanna Bitton, Manish Bhatt, Cristian Canton Ferrer, Aaron Grattafiori, Wenhan Xiong, Alexandre Défossez, and 7 others. 2024. [Code llama: Open foundation models for code](#). *Preprint*, arXiv:2308.12950.
- Rachel Rudinger, Jason Naradowsky, Brian Leonard, and Benjamin Van Durme. 2018. [Gender bias in coreference resolution](#). *Preprint*, arXiv:1804.09301.
- Keisuke Sakaguchi, Ronan Le Bras, Chandra Bhagavatula, and Yejin Choi. 2019. [Winogrande: An adversarial winograd schema challenge at scale](#). *Preprint*, arXiv:1907.10641.
- Maarten Sap, Hannah Rashkin, Derek Chen, Ronan LeBras, and Yejin Choi. 2019. [Socialliqa: Commonsense reasoning about social interactions](#). *Preprint*, arXiv:1904.09728.
- Akira Sasaki, Masato Hirakawa, Shintaro Horie, and Tomoaki Nakamura. 2023. [Elyza-japanese-llama-2-7b](#).
- Kei Sawada, Tianyu Zhao, Makoto Shing, Kentaro Mitsui, Akio Kaga, Yukiya Hono, Toshiaki Wakatsuki, and Koh Mitsuda. 2024. [Release of pre-trained models for the japanese language](#). *Preprint*, arXiv:2404.01657.
- Noam Shazeer. 2019. [Fast transformer decoding: One write-head is all you need](#). *Preprint*, arXiv:1911.02150.
- Sidak Pal Singh, Bobby He, Thomas Hofmann, and Bernhard Schölkopf. 2025. [The directionality of optimization trajectories in neural networks](#). In *The Thirteenth International Conference on Learning Representations, ICLR 2025, Singapore, April 24-28, 2025*. OpenReview.net.

- Karan Singhal, Shekoofeh Azizi, Tao Tu, S. Sara Mahdavi, Jason Wei, Hyung Won Chung, Nathan Scales, Ajay Tanwani, Heather Cole-Lewis, Stephen Pfohl, Perry Payne, Martin Seneviratne, Paul Gamble, Chris Kelly, Nathaneal Scharli, Aakanksha Chowdhery, Philip Mansfield, Blaise Aguera y Arcas, Dale Webster, and 11 others. 2022. [Large language models encode clinical knowledge](#). *Preprint*, arXiv:2212.13138.
- Karan Singhal, Tao Tu, Juraj Gottweis, Rory Sayres, Ellery Wulczyn, Le Hou, Kevin Clark, Stephen Pfohl, Heather Cole-Lewis, Darlene Neal, Mike Schaeckermann, Amy Wang, Mohamed Amin, Sami Lachgar, Philip Mansfield, Sushant Prakash, Bradley Green, Ewa Dominowska, Blaise Aguera y Arcas, and 12 others. 2023. [Towards expert-level medical question answering with large language models](#). *Preprint*, arXiv:2305.09617.
- Aarohi Srivastava, Abhinav Rastogi, Abhishek Rao, Abu Awal Md Shoeb, Abubakar Abid, Adam Fisch, Adam R. Brown, Adam Santoro, Aditya Gupta, Adrià Garriga-Alonso, Agnieszka Kluska, Aitor Lewkowycz, Akshat Agarwal, Alethea Power, Alex Ray, Alex Warstadt, Alexander W. Kocurek, Ali Safaya, Ali Tazarv, and 432 others. 2023. [Beyond the imitation game: Quantifying and extrapolating the capabilities of language models](#). *Preprint*, arXiv:2206.04615.
- Jianlin Su, Yu Lu, Shengfeng Pan, Ahmed Murtadha, Bo Wen, and Yunfeng Liu. 2023. [Roformer: Enhanced transformer with rotary position embedding](#). *Preprint*, arXiv:2104.09864.
- Shivchander Sudalairaj, Abhishek Bhandwadar, Aldo Pareja, Kai Xu, David D. Cox, and Akash Srivastava. 2024. [Lab: Large-scale alignment for chatbots](#). *Preprint*, arXiv:2403.01081.
- Alon Talmor, Jonathan Herzig, Nicholas Lourie, and Jonathan Berant. 2019. [Commonsenseqa: A question answering challenge targeting commonsense knowledge](#). *Preprint*, arXiv:1811.00937.
- "Teknium", Charles Goddard, "interstellarninja", "theemozilla", "karan4d", and "huemin_art". 2024a. [Hermes-2-theta-llama-3-8b](#).
- "Teknium", "interstellarninja", "theemozilla", "karan4d", and "huemin_art". 2024b. [Hermes-2-pro-llama-3-8b](#).
- "Teknium", "theemozilla", "karan4d", and "huemin_art". 2024c. [Nous hermes 2 mistral 7b dpo](#).
- Together Computer. 2023. [Redpajama-data: An open source recipe to reproduce llama training dataset](#).
- Hugo Touvron, Thibaut Lavril, Gautier Izacard, Xavier Martinet, Marie-Anne Lachaux, Timothée Lacroix, Baptiste Rozière, Naman Goyal, Eric Hambro, Faisal Azhar, Aurelien Rodriguez, Armand Joulin, Edouard Grave, and Guillaume Lample. 2023a. [Llama: Open and efficient foundation language models](#). *Preprint*, arXiv:2302.13971.
- Hugo Touvron, Louis Martin, Kevin Stone, Peter Albert, Amjad Almahairi, Yasmine Babaei, Nikolay Bashlykov, Soumya Batra, Prajjwal Bhargava, Shruti Bhosale, Dan Bikel, Lukas Blecher, Cristian Canton Ferrer, Moya Chen, Guillem Cucurull, David Esiobu, Jude Fernandes, Jeremy Fu, Wenyin Fu, and 49 others. 2023b. [Llama 2: Open foundation and fine-tuned chat models](#). *Preprint*, arXiv:2307.09288.
- Lewis Tunstall, Edward Beeching, Nathan Lambert, Nazneen Rajani, Kashif Rasul, Younes Belkada, Shengyi Huang, Leandro von Werra, Clémentine Fourrier, Nathan Habib, Nathan Sarrazin, Omar Sanseviero, Alexander M. Rush, and Thomas Wolf. 2023. [Zephyr: Direct distillation of lm alignment](#). *Preprint*, arXiv:2310.16944.
- Laurens van der Maaten and Geoffrey Hinton. 2008. [Visualizing data using t-sne](#). *Journal of Machine Learning Research*, 9(86):2579–2605.
- Oskar van der Wal, Pietro Lesci, Max Müller-Eberstein, Naomi Saphra, Hailey Schoelkopf, Willem Zuidema, and Stella Biderman. 2025. [Polypythias: Stability and outliers across fifty language model pre-training runs](#). In *The Thirteenth International Conference on Learning Representations*.
- Ben Wang. 2021. [Mesh-Transformer-JAX: Model-Parallel Implementation of Transformer Language Model with JAX](#).
- Ben Wang and Aran Komatsuzaki. 2021. [GPT-J-6B: A 6 Billion Parameter Autoregressive Language Model](#).
- Guan Wang, Sijie Cheng, Xianyuan Zhan, Xiangang Li, Sen Song, and Yang Liu. 2024a. [Openchat: Advancing open-source language models with mixed-quality data](#). *Preprint*, arXiv:2309.11235.
- Shenzhi Wang, Yaowei Zheng, Guoyin Wang, Shiji Song, and Gao Huang. 2024b. [Llama3-8b-chinese-chat \(revision 6622a23\)](#).
- Chris Wendler, Veniamin Veselovsky, Giovanni Monea, and Robert West. 2024. [Do llamas work in english? on the latent language of multilingual transformers](#). In *Proceedings of the 62nd Annual Meeting of the Association for Computational Linguistics (Volume 1: Long Papers), ACL 2024, Bangkok, Thailand, August 11-16, 2024*, pages 15366–15394. Association for Computational Linguistics.
- Huajian Xin, Z. Z. Ren, Junxiao Song, Zhihong Shao, Wanxia Zhao, Haocheng Wang, Bo Liu, Liyue Zhang, Xuan Lu, Qiushi Du, Wenjun Gao, Qihao Zhu, Dejian Yang, Zhibin Gou, Z. F. Wu, Fuli Luo, and Chong Ruan. 2024. [Deepseek-prover-v1.5: Harnessing proof assistant feedback for reinforcement learning and monte-carlo tree search](#). *Preprint*, arXiv:2408.08152.
- Haoran Xu, Young Jin Kim, Amr Sharaf, and Hany Hassan Awadalla. 2024a. [A paradigm shift in machine translation: Boosting translation performance of large language models](#). *Preprint*, arXiv:2309.11674.

Haoran Xu, Amr Sharaf, Yunmo Chen, Weiting Tan, Lingfeng Shen, Benjamin Van Durme, Kenton Murray, and Young Jin Kim. 2024b. [Contrastive preference optimization: Pushing the boundaries of llm performance in machine translation](#). *Preprint*, arXiv:2401.08417.

An Yang, Baosong Yang, Binyuan Hui, Bo Zheng, Bowen Yu, Chang Zhou, Chengpeng Li, Chengyuan Li, Dayiheng Liu, Fei Huang, Guanting Dong, Haoran Wei, Huan Lin, Jialong Tang, Jialin Wang, Jian Yang, Jianhong Tu, Jianwei Zhang, Jianxin Ma, and 43 others. 2024. [Qwen2 technical report](#). *Preprint*, arXiv:2407.10671.

Longhui Yu, Weisen Jiang, Han Shi, Jincheng Yu, Zhengying Liu, Yu Zhang, James T. Kwok, Zhenguo Li, Adrian Weller, and Weiyang Liu. 2024. [Metamath: Bootstrap your own mathematical questions for large language models](#). *Preprint*, arXiv:2309.12284.

Rowan Zellers, Ari Holtzman, Yonatan Bisk, Ali Farhadi, and Yejin Choi. 2019. [Hellswag: Can a machine really finish your sentence?](#) *Preprint*, arXiv:1905.07830.

Susan Zhang, Stephen Roller, Naman Goyal, Mikel Artetxe, Moya Chen, Shuohui Chen, Christopher Dewan, Mona Diab, Xian Li, Xi Victoria Lin, Todor Mihaylov, Myle Ott, Sam Shleifer, Kurt Shuster, Daniel Simig, Punit Singh Koura, Anjali Sridhar, Tianlu Wang, and Luke Zettlemoyer. 2022. [Opt: Open pre-trained transformer language models](#). *Preprint*, arXiv:2205.01068.

Jieyu Zhao, Tianlu Wang, Mark Yatskar, Vicente Ordonez, and Kai-Wei Chang. 2018. [Gender bias in coreference resolution: Evaluation and debiasing methods](#). *Preprint*, arXiv:1804.06876.

Tianyu Zhao, Akio Kaga, and Kei Sawada. 2023. [rinna/yourri-7b](#).

Lianmin Zheng, Wei-Lin Chiang, Ying Sheng, Siyuan Zhuang, Zhanghao Wu, Yonghao Zhuang, Zi Lin, Zhuohan Li, Dacheng Li, Eric P. Xing, Hao Zhang, Joseph E. Gonzalez, and Ion Stoica. 2023. [Judging llm-as-a-judge with mt-bench and chatbot arena](#). *Preprint*, arXiv:2306.05685.

Wanjun Zhong, Ruixiang Cui, Yiduo Guo, Yaobo Liang, Shuai Lu, Yanlin Wang, Amin Saied, Weizhu Chen, and Nan Duan. 2023. [Agieval: A human-centric benchmark for evaluating foundation models](#). *Preprint*, arXiv:2304.06364.

A Related Work on Oscillatory Trajectories in Weight Space

We analyzed model trajectories in the log-likelihood space, where each model was represented by its output probabilities on a fixed text set. This space reflects the model’s behavior directly,

and our study was, to the best of our knowledge, the first to reveal structural patterns in training dynamics within this representation. In particular, we observed the emergence of spiral-shaped trajectories as well as indications of constrained diffusion, which we further examine in Appendix B.

While our main focus was on the log-likelihood space, we also briefly examined model trajectories in weight space for comparison (Appendix D.5). As shown in Fig. 16, oscillatory behavior was also observed in the weight space during the later stages of training. Although the patterns differed in periodicity and structure, the presence of oscillations in both spaces suggests a potentially broader phenomenon in the dynamics of neural networks. The observed difference may reflect the presence of multiple modes of variation, with different modes being emphasized in the weight and output spaces.

To contextualize these findings, we review prior work that has reported oscillatory behaviors in weight space during training. The *Edge of Stability* phenomenon (Cohen et al., 2021; Arora et al., 2022) refers to the behavior of training loss oscillating while decreasing, observed when gradient descent enters an unstable region where the largest Hessian eigenvalue hovers near the critical learning rate. Singh et al. (2025) observed micro-level oscillations in training trajectories through changes in the cosine similarity of weights. Netay (2024) empirically identified double-helical trajectories in neural network weights, noting a relationship between these trajectories’ periodicity and the hyperparameters of the Adam optimizer. Kunin et al. (2024) found that weights exhibit anomalous diffusion after convergence and demonstrated oscillatory dynamics in the weight phase space, governed by the eigenstructure of the Hessian of the loss function.

B Related Work and Discussions on Diffusion Exponents

In Section 3, we estimated the diffusion exponents c_w and c_q corresponding to the trajectories of models in weight and log-likelihood spaces, respectively. Our analysis revealed that during the early phase of training, both exponents are relatively large ($c_w = 1.2$ and $c_q = 0.8$), but they decrease as training progresses. At the later stages, the exponent in weight space approaches $c_w \approx 1$, which corresponds to Brownian motion, while the exponent in log-likelihood space becomes significantly

smaller ($c_q \ll 1$), which is characteristic of subdiffusion.

In our experimental setting, texts were sampled from a corpus that closely approximates the training data. Consequently, each element of the log-likelihood vector represents a term contributing to the cross-entropy loss, and the negative average of these terms serves as an unbiased estimator of the expected loss. The contrast between the relatively large diffusion exponent in weight space and the much smaller exponent in log-likelihood space suggests that even as model weights continue to change, the output probabilities remain stable. As a result, the loss function is largely unaffected by these weight changes. This observation aligns with the hypothesis that stochastic gradient descent favors flat minima (Keskar et al., 2017).

Moreover, near the loss minima, the sum of negative log-likelihoods is constrained as cross-entropy loss, implying convergence to regions where many texts have high log-likelihood values. The observed small diffusion exponent suggests that the movement of the vectors becomes restricted in these regions.

C Standard Error of the Estimated KL Divergence

Let \mathbf{q}_i and \mathbf{q}_j denote the \mathbf{q} coordinates of models p_i and p_j , respectively. While we use \mathbf{q} pre-scaled by $1/\sqrt{N}$ in the main body of this paper, we do not apply this scaling in this appendix. Accordingly, the KL divergence between the models is estimated as $\text{KL}(p_i, p_j) \approx \frac{1}{N} \|\mathbf{q}_i - \mathbf{q}_j\|^2 = \frac{1}{N} \sum_{k=1}^N (Q_{ik} - Q_{jk})^2$, which corresponds to the sample mean of $\{(Q_{ik} - Q_{jk})^2\}_{k=1}^N$. Assuming that the effects of double-centering in \mathbf{Q} are negligible, these terms can be treated as approximately independent. When N is sufficiently large, the variance of the estimated KL divergence is given by

$$\begin{aligned} \text{Var}(\text{KL}(p_i, p_j)) &\approx \frac{1}{N} \left\{ \frac{1}{N} \sum_{k=1}^N (Q_{ik} - Q_{jk})^4 - \frac{1}{N^2} \|\mathbf{q}_i - \mathbf{q}_j\|^4 \right\} \\ &\approx \frac{1}{N^2} \sum_{k=1}^N (Q_{ik} - Q_{jk})^4 - \frac{1}{N} \text{KL}(p_i, p_j)^2. \end{aligned}$$

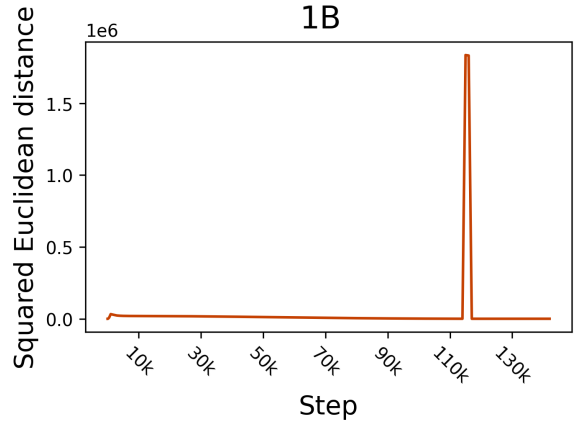


Figure 8: Squared Euclidean distance between the weights of consecutive checkpoints for Pythia 1B. The distances between 115k and 116k, and between 116k and 117k are abnormally large.

Therefore, the standard error of the estimator $\text{KL}(p_i, p_j)$ can be approximated as

$$\begin{aligned} \text{SE}(\text{KL}(p_i, p_j)) &\approx \sqrt{\frac{1}{N^2} \sum_{k=1}^N (Q_{ik} - Q_{jk})^4 - \frac{1}{N} \text{KL}(p_i, p_j)^2}. \end{aligned}$$

D Details of Section 3

To analyze the trajectories of language models during pretraining, we used Pythia models⁶ of various sizes, as listed in Table 5 in Appendix G. For each checkpoint, we computed log-likelihood vectors using the same set of 10,000 texts as in Oyama et al. (2025). The computations were performed on an NVIDIA RTX 6000 Ada and took approximately 10 minutes for a 7B model loaded in float16 precision.

D.1 Preprocessing

Assuming that the KL divergence between consecutive checkpoints changes smoothly, we regarded certain checkpoints and texts as outliers. All experiments were conducted after removing these outliers. This appendix provides a detailed description of the preprocessing procedure.

Removing outlier models. As shown in Fig. 8, the Euclidean distance between weights near step 116k of Pythia 1B is abnormally large. We suspect that this checkpoint may not have been saved properly and therefore excluded it from our analysis. A question about this checkpoint was also raised on

⁶Released under the Apache 2.0 License.

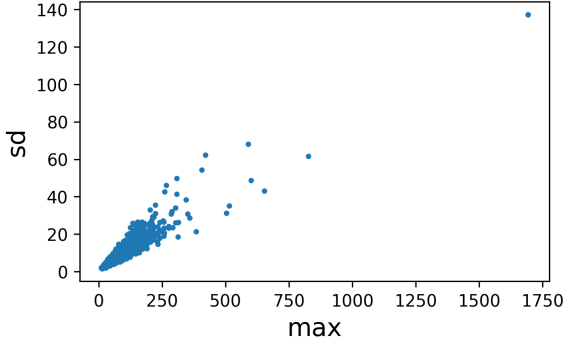


Figure 9: The relationship between the maximum and the standard deviation of the absolute differences in log-likelihoods between consecutive checkpoints of the same model size, computed for each text.

the Discussions page of the Pythia 1B model on Hugging Face⁷.

Removing outlier texts. Following Oyama et al. (2025), we clip the log-likelihood matrix L at the bottom 2%, after excluding the outlier model. Next, we consider the log-likelihood difference for each text between consecutive checkpoints after the warmup phase. For each text, we define its outlier score as the maximum absolute difference across all model sizes and training steps. Specifically, letting $p_{i,t}$ denote the model of size i at step t , the outlier score for a text x is given by $\max_{i,t} \{|p_{i,t+1}(x) - p_{i,t}(x)|\}$. It is also possible to assign scores to texts using the standard deviation of these differences. However, Fig. 9 shows that the maximum and the standard deviation are highly correlated. Therefore, we adopt the maximum value for scoring. The figure further confirms the presence of texts that clearly behave as outliers. For example, the text with the highest outlier score was a meaningless and repetitive sequence of symbols, such as `028a28a0028a28a0028a28a...`

Fig. 10 shows the KL divergence between consecutive checkpoints after step 10k⁸, plotted as a function of the number of top outlier-scored texts removed (top 10, 100, 200, ..., 1000). When the top 300 texts (3%) are removed, the variation in KL divergence stabilizes with respect to the number of removed texts. Therefore, we excluded these 300 texts from our experiments.

⁷<https://huggingface.co/EleutherAI/pythia-1b/discussions/4>

⁸The maximum is computed from step 2k onward, after the warmup phase, but we visualize from step 10k to better capture the variation in KL divergence.

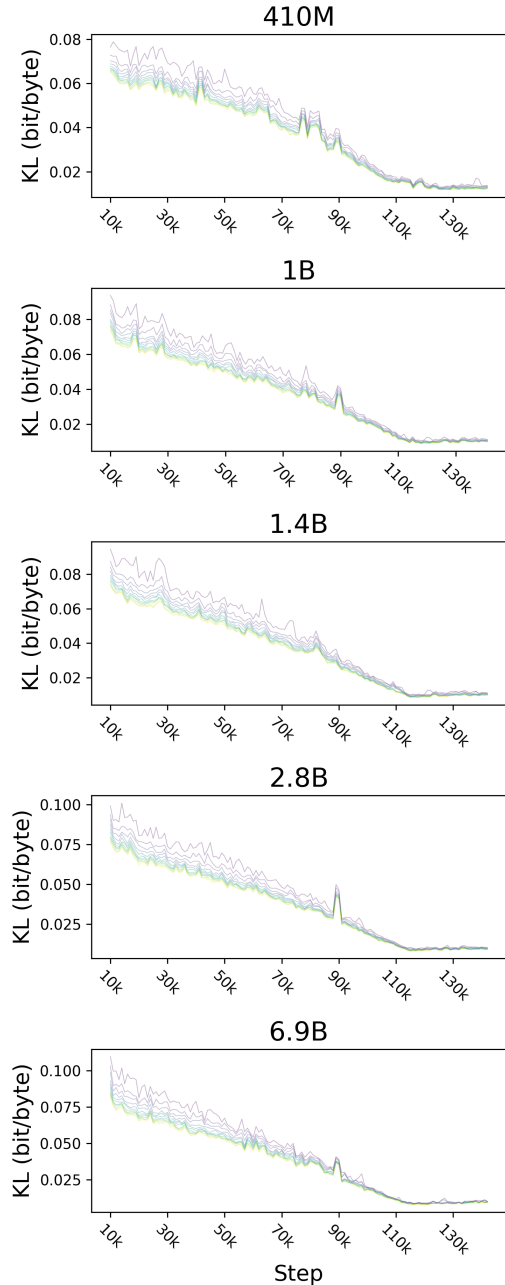
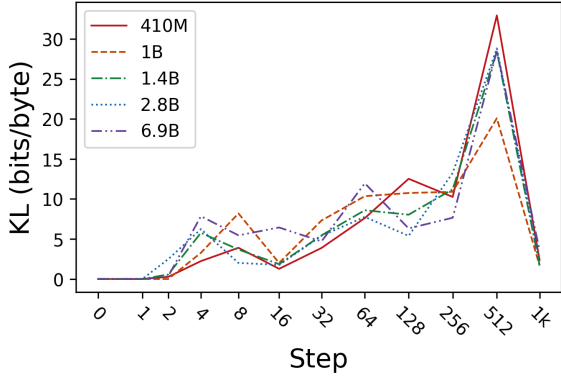


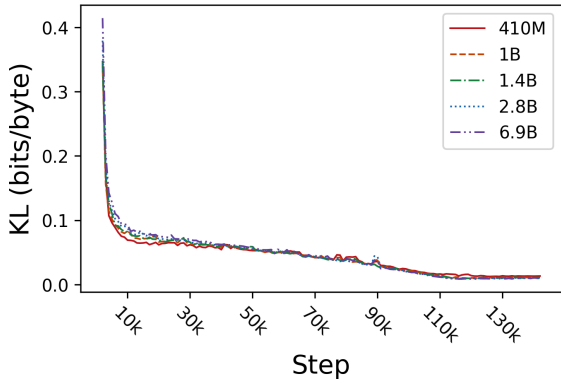
Figure 10: Change in KL divergence after step 10k as a function of the number of top outlier texts removed (10, 100, 200, ..., 1000). Brighter colors indicate larger numbers of removed texts.

D.2 KL Divergence between Checkpoints

Fig. 11 shows the variation in KL divergence between consecutive checkpoints for all model sizes. In this figure, the value at step 10k, for example, represents the KL divergence between the checkpoints at steps 10k and 11k. During pretraining, the learning rate changes dynamically with the training step. In particular, the first 1,430 steps correspond to the warmup phase, during which the



(a) KL divergence between consecutive checkpoints during the warmup phase. The horizontal axis is scaled as $\log_{10}(1 + \text{Step})$.



(b) KL divergence between consecutive checkpoints after the warmup phase. When the vertical axis is plotted on a logarithmic scale, this corresponds to the right panel of Fig. 4.

Figure 11: KL divergence between consecutive checkpoints of Pythia. For example, the value at step 10k on the horizontal axis represents the KL divergence between the checkpoints at steps 10k and 11k.

learning rate increases linearly. As a result, as shown in Fig. 11a, the KL divergence between the checkpoints takes on relatively large values, mostly exceeding 10 bit/byte during this interval. Additionally, Fig. 12 plots the KL divergence between consecutive checkpoints after step 10k for Pythia, along with the corresponding standard error. The derivation of the standard error is described in Appendix C. Finally, Table 3 presents the pairwise KL divergence between model sizes at the final checkpoint. As discussed in Section 3, the divergence caused by differences in model size is larger than that resulting from 1k steps of training.

D.3 Period of Spiral Trajectory

In this appendix, we describe the procedure used to analyze the spiral trajectories suggested in Fig. 1. For each model size in Pythia, 3D t-SNE is applied

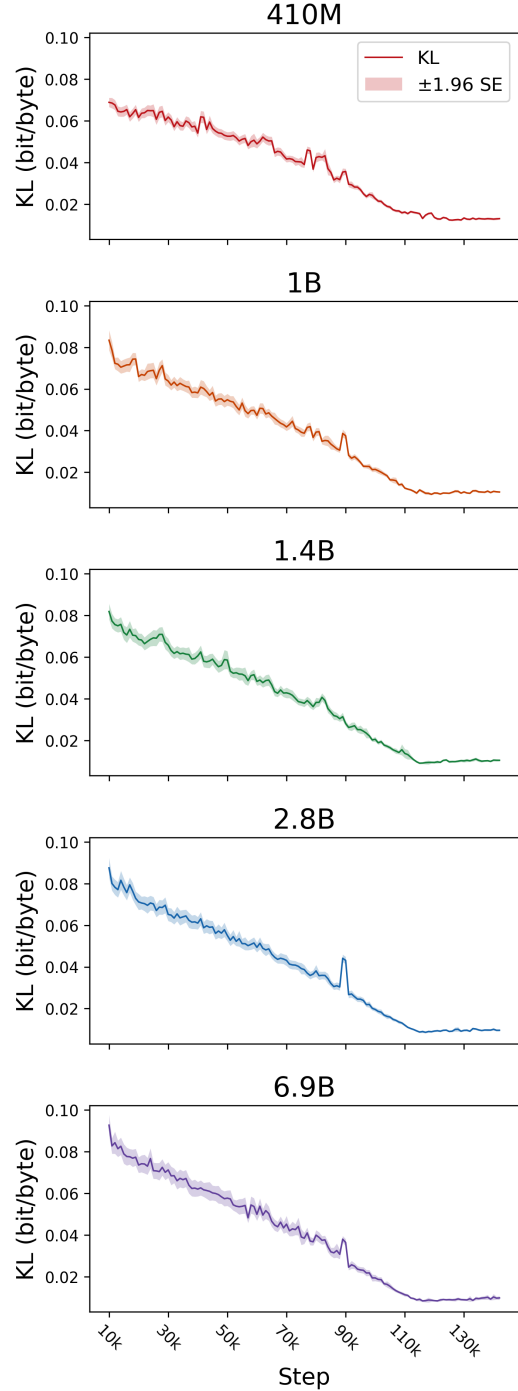


Figure 12: KL divergence and its standard error between consecutive checkpoints of Pythia after step 10k.

independently. PCA is then performed on the sequence of checkpoints from the midpoint of the trajectory (step 67k onward) to extract principal axes. Since PC1 corresponds to the overall direction of trajectory progression, we plot PC2 versus PC3 in the left panel of Fig. 13, where the trajectory approximately forms a circular pattern. We also compute the autocorrelation function of the PC3 values, treated as a time series, and show the result

	410M	1B	1.4B	2.8B	6.9B
410M	0.00	0.28	0.52	1.04	1.7
1B	0.28	0.00	0.15	0.44	0.92
1.4B	0.52	0.15	0.00	0.21	0.57
2.8B	1.0	0.44	0.21	0.00	0.21
6.9B	1.7	0.92	0.57	0.21	0.00

Table 3: KL divergence (bit/byte) between different model sizes at the final checkpoint of Pythia.

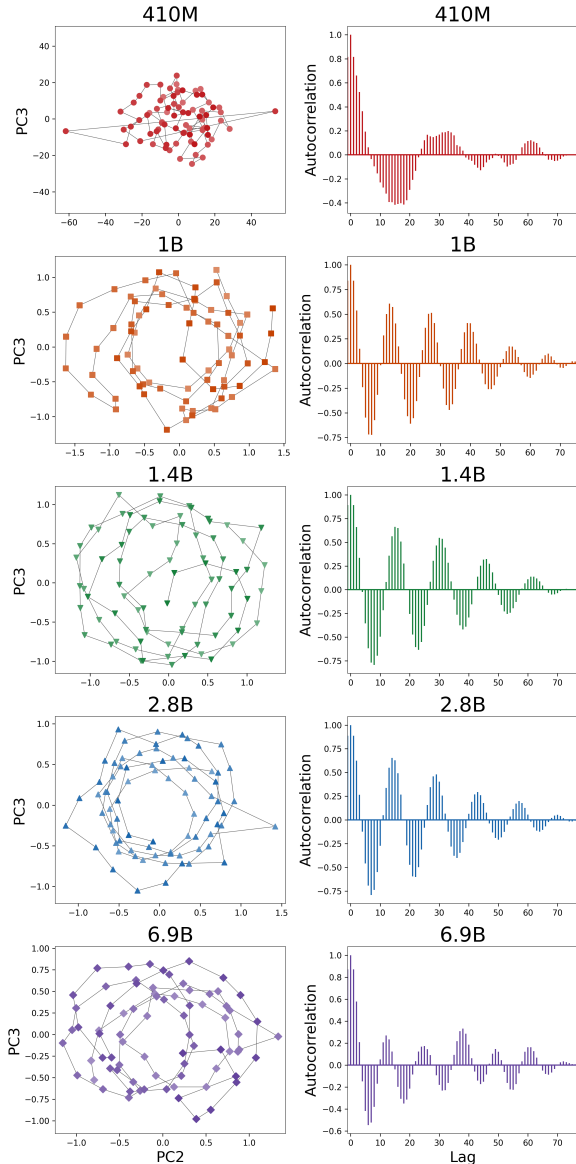


Figure 13: (Left) PC2 vs. PC3 after applying PCA to the later half portion of the 3D t-SNE trajectories for each Pythia model size. (Right) Autocorrelation function of PC3.

in the right panel of Fig. 13. The spiral period reported in Table 2 is defined as the step at which the autocorrelation reaches its maximum between the second and third zero-crossings.

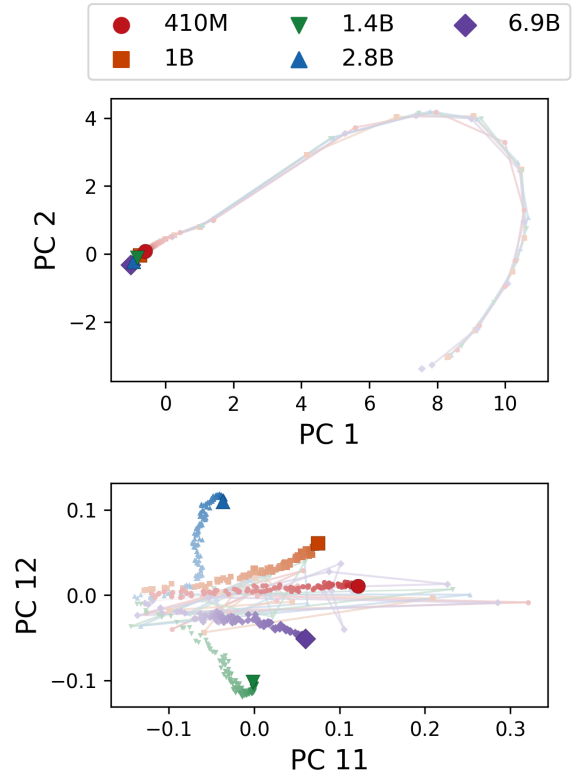


Figure 14: PCA visualization of the training trajectories of Pythia models. (Top) PC1 vs. PC2. (Bottom) PC11 vs. PC12.

D.4 PCA

In Section 3, we visualized the trajectories of Pythia during pretraining using t-SNE. In this appendix, we instead visualize the trajectories using PCA.

Fig. 14 shows the result of applying PCA simultaneously to all model sizes and plotting their trajectories. Fig. 15 further illustrates the evolution of multiple principal component values along the training steps. Unlike t-SNE, the top principal components exhibit similar values across model sizes, resulting in overlapping trajectories. This difference likely arises from the fact that the top principal components capture global variation in the trajectories, whereas t-SNE emphasizes local structure. In contrast, the lower principal components exhibit more noise-like behavior. As shown in Table 3, the KL divergence between different model sizes at the final checkpoint is larger than that between consecutive checkpoints. This is consistent with the observation that trajectories are separated in the lower components.

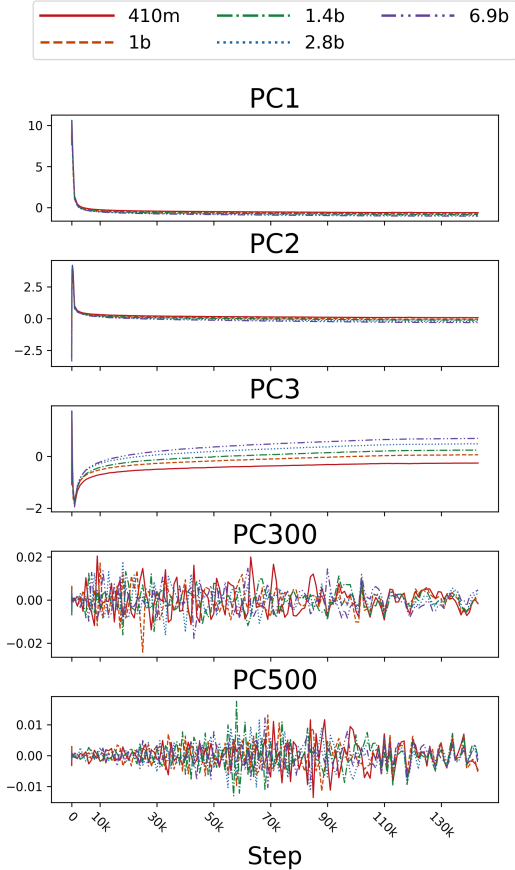


Figure 15: Variation of principal component values from PCA applied to the trajectories of all Pythia model sizes.

D.5 Comparison with Weights

This appendix describes the procedure for comparing language models using the Euclidean distance between the weights of Pythia checkpoints.

Trajectory. For each model size, we computed a distance matrix containing the pairwise Euclidean distances among all checkpoints. Fig. 16 shows the trajectories from step 100k onward, visualized using t-SNE⁹. The trajectories were centered after t-SNE to align the plot ranges. In addition, for the 1B model, the trajectory was rotated by 180 degrees to align its rough direction of progression with that of the other model sizes.

Anomalous diffusion. Fig. 3 shows the evolution of squared Euclidean distances in weights and log-likelihood vectors over 10k steps starting from step 120k. Fig. 4 illustrates how the estimated diffusion exponent changes when varying the starting step for the calculation. To ensure stability, we vary the starting point only after the warmup phase. The exponent is estimated using linear regression

⁹t-SNE can take a distance matrix as input.

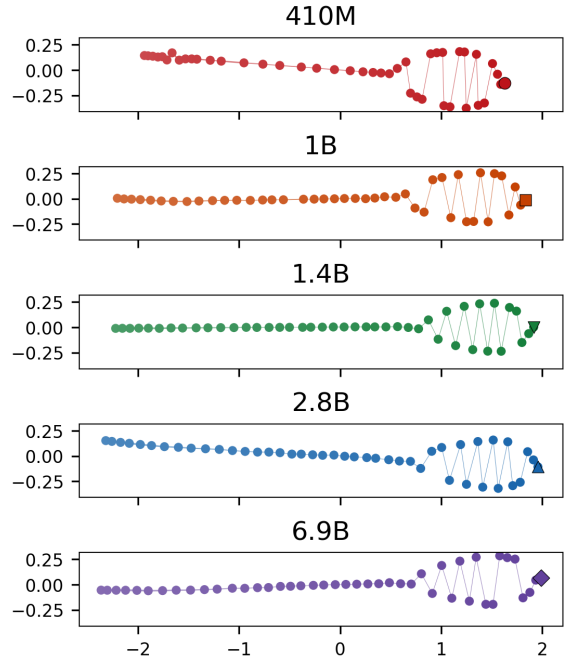


Figure 16: t-SNE visualization of the trajectories based on weight-space distances for Pythia models after step 100k. To align scales across model sizes, the trajectories were centered after t-SNE. They were also rotated to align the directions of progression. Final checkpoints are indicated using distinct markers.

(least squares) over a 10k-step window beginning at each initial step. Summary statistics of the coefficient of determination (R^2) for each regression are provided in Table 4.

D.6 Different Seeds

van der Wal et al. (2025) trained Pythia models with nine different seeds and released checkpoints at the same steps as in the original Pythia suite. The random seed affects the initialization of weights and the order of the training data. We used all available checkpoints for the 410M models with seeds 1 through 9. However, at the time of writing this paper, the weights for (seed, step) = (2, 111k), (6, 88k), and (9, 40k) were not available on Hugging Face and were therefore excluded from our analysis¹⁰. The original 410M model was trained with seed 1234.

Fig. 17 shows the KL divergence between the final checkpoints of models trained with different seeds. Despite sharing the same architecture and data, the KL divergence between seed 3 and the other seeds, as well as between seed 4 and the oth-

¹⁰For example, see <https://huggingface.co/EleutherAI/pythia-410m-seed2/tree/step111000>.

Size	Log-likelihood	Weight
410M	0.849	0.993
	(± 0.158)	(± 0.00622)
1B	0.935	0.999
	(± 0.0866)	(± 0.000922)
1.4B	0.955	0.999
	(± 0.0336)	(± 0.000687)
2.8B	0.959	0.999
	(± 0.088)	(± 0.000704)
6.9B	0.977	0.999
	(± 0.0305)	(± 0.000975)

Table 4: The mean and standard deviation of the coefficient of determination (R^2) when varying the starting step used to compute the diffusion exponent.

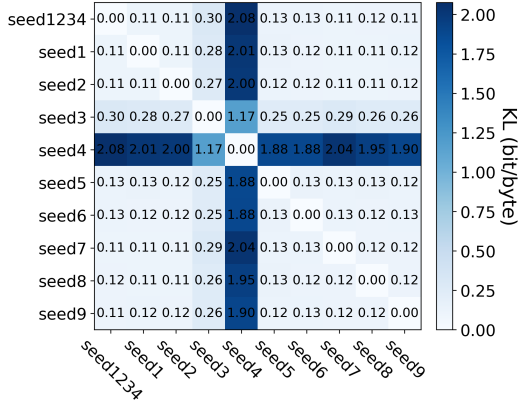


Figure 17: KL divergence between the final checkpoints of Pythia 410M models with different seeds.

ers, are significantly larger. According to van der Wal et al. (2025), models trained with seed 3 and seed 4 experienced loss spikes during training and are considered outliers in terms of performance. This suggests that KL divergence is also effective in identifying such outlier models. Therefore, seed 3 and seed 4 are excluded when generating Fig. 1. We also report in Table 1a the average KL divergence between the final checkpoint of the original 410M model and those of seeds 1, 2, 5, 6, 7, 8, and 9.

E Details of Section 4

We describe the language models used in Section 4. From the 1,018 models analyzed in Oyama et al. (2025), we identified fine-tuned models as those whose base model is specified in the metadata available via the Hugging Face Hub API¹¹. Our analysis was conducted on pairs of fine-tuned models and their base models. Models associated with multiple base models (i.e., merged models) were excluded. A list of the language models used in this analysis

¹¹https://github.com/huggingface/huggingface_hub

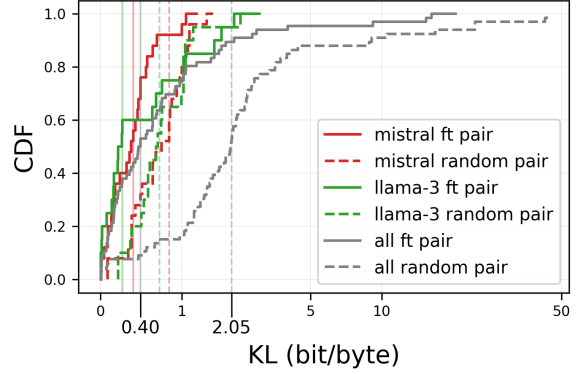


Figure 18: Cumulative distribution of KL divergence for pairs of fine-tuned models and their base models, and for randomly selected model pairs (corresponding to Table 1b). The horizontal axis is scaled as $\log_{10}(1 + \text{KL})$. The dotted lines indicate the median of each distribution.

is provided in Table 6 in Appendix G. In Fig. 5, there are a few pairs connected by line segments that span across different colors, namely different model types. This occurs because, under the model type classification method used in Oyama et al. (2025), some fine-tuned models were categorized as belonging to the “others” type. In our experiments, when we refer to, for example, a “llama-3 fine-tuned pair”, we mean a pair in which the fine-tuned model is of the llama-3 type.

Fig. 18 illustrates the cumulative distributions of KL divergence for pairs of fine-tuned models and their base pairs, as well as for randomly selected model pairs. Summary statistics for these distributions are reported in Table 1b. The figure shows that KL divergence after fine-tuning tends to be slightly smaller, as indicated by the left-skewed distribution. As noted in Oyama et al. (2025), models of the same type tend to have smaller KL divergence. To more accurately assess the effect of fine-tuning, we also analyze random model pairs sampled within the same model type.

F Details of Section 5

Here, we describe the language models used in Section 5. For the trajectories shown in Fig. 6 and Fig. 19, we selected the 50 most downloaded models from those analyzed in Oyama et al. (2025). For specified model type analysis, we selected models with 32 layers from the llama-2, llama-3, and mistral types. For each of these types, we used the 10 most downloaded models. These models were used in the analysis shown in Fig. 7 and Fig. 20. A

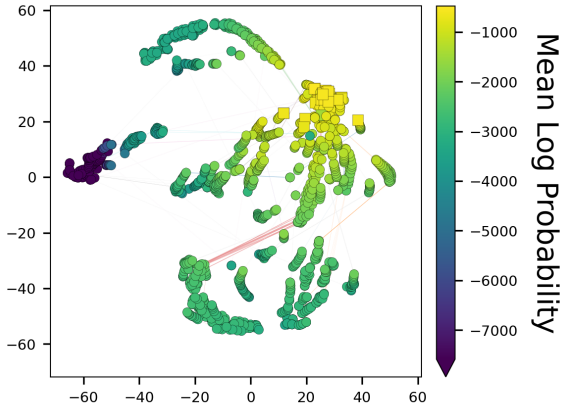


Figure 19: Re-rendering of the top panel of Fig. 6. Colors indicate mean log-likelihood, clipped at the bottom 5% across all values to improve visibility.

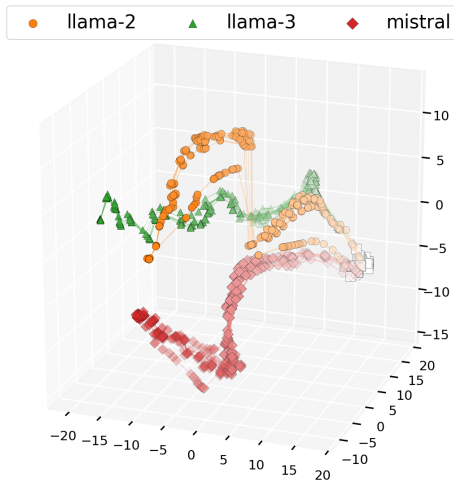


Figure 20: 3D t-SNE visualization of the left panel of Fig. 7. Deeper layers are represented with lighter colors, and the final layer is indicated by a white square.

complete list of the models is provided in Table 7 in Appendix G.

Fig. 19 shows the trajectories of models across layers, color-coded by mean log-likelihood, depending on layer depth. The mean log-likelihood increases as the layer depth increases. This indicates that the direction of trajectory progression corresponds to deeper layers, that is, to increasing mean log-likelihood. Additionally, Fig. 20 presents a 3D version of the left panel of Fig. 6. This illustration implies that the jump observed in Fig. 7 is not an artifact of the 2D t-SNE visualization, but rather results from a genuinely large KL divergence between adjacent layers.

G Model List

The models used in Sections 3, 4, and 5 are listed in Tables 5, 6, and 7, respectively. Table 5 is sorted by model size; Table 6 is sorted alphabetically by model name, considering the model generation, model type, and corresponding base model; and Table 7 is sorted in descending order of download counts.

BibTeX entries for each model were selected according to the procedure described by Oyama et al. (2025). Note that, for the Pythia models trained with different random seeds (van der Wal et al., 2025) and used in Section 3, the corresponding BibTeX entries in Table 5 were prepared manually.

Table 5: List of 14 models in the experiments for pretraining models. “ID” denotes the index sorted by model size; “Model Name” denotes the name of the model.

ID	Model Name
1	EleutherAI/pythia-410m (Gao et al., 2020; Biderman et al., 2022, 2023)
2	EleutherAI/pythia-410m-seed1 (van der Wal et al., 2025)
3	EleutherAI/pythia-410m-seed2 (van der Wal et al., 2025)
4	EleutherAI/pythia-410m-seed3 (van der Wal et al., 2025)
5	EleutherAI/pythia-410m-seed4 (van der Wal et al., 2025)
6	EleutherAI/pythia-410m-seed5 (van der Wal et al., 2025)
7	EleutherAI/pythia-410m-seed6 (van der Wal et al., 2025)
8	EleutherAI/pythia-410m-seed7 (van der Wal et al., 2025)
9	EleutherAI/pythia-410m-seed8 (van der Wal et al., 2025)
10	EleutherAI/pythia-410m-seed9 (van der Wal et al., 2025)
11	EleutherAI/pythia-1b (Gao et al., 2020; Biderman et al., 2022, 2023)
12	EleutherAI/pythia-1.4b (Gao et al., 2020; Biderman et al., 2022, 2023)
13	EleutherAI/pythia-2.8b (Gao et al., 2020; Biderman et al., 2022, 2023)
14	EleutherAI/pythia-6.9b (Gao et al., 2020; Biderman et al., 2022, 2023)

Table 6: List of 87 models in the experiments for fine-tuning models. “ID” denotes the alphabetical index considering the generation and the base model; “Model Name” denotes the name of the model; “Base Model Name” denotes the name of the base model before training; “Model Type” denotes the model classification defined in Oyama et al. (2025); “Generation” denotes the model generation in the training process; “DLs” denotes the total number of downloads.

ID	Model Name	Base Model Name	Model Type	Generation	DLs
1	deepseek-ai/DeepSeek-Prover-V1.5-Base (Xin et al., 2024)	–	deepseek	1	230
2	tiuae/falcon-rw-1b (Brown et al., 2020; Press et al., 2022; Dao et al., 2022; Penedo et al., 2023)	–	falcon	1	22921
3	google/gemma-1.1-7b-it (Joshi et al., 2017; Mihaylov et al., 2018; Zhao et al., 2018; Clark et al., 2019; Talmor et al., 2019; Sap et al., 2019; Sakaguchi et al., 2019; Bisk et al., 2019; Chollet, 2019; Zellers et al., 2019; Hendrycks et al., 2021; Chen et al., 2021; Austin et al., 2021; Cobbe et al., 2021; Parrish et al., 2022; Srivastava et al., 2023; Zhong et al., 2023; Gemini Team et al., 2024)	–	gemma	1	19835
4	google/gemma-7b (Joshi et al., 2017; Mihaylov et al., 2018; Zhao et al., 2018; Rudinger et al., 2018; Bisk et al., 2019; Chollet, 2019; Clark et al., 2019; Talmor et al., 2019; Sap et al., 2019; Zellers et al., 2019; Sakaguchi et al., 2019; Gehman et al., 2020; Chen et al., 2021; Austin et al., 2021; Hendrycks et al., 2021; Dhamala et al., 2021; Cobbe et al., 2021; Lin et al., 2022; Hartvigsen et al., 2022; Parrish et al., 2022; Srivastava et al., 2023; Zhong et al., 2023; Detmers et al., 2023; Gemini Team et al., 2024)	–	gemma	1	72047
5	openchat/openchat-3.5-0106-gemma (Wang et al., 2024a)	–	gemma	1	7817
6	openlm-research/open_llama_3b (Together Computer, 2023; Touvron et al., 2023a; Geng and Liu, 2023)	–	llama-1	1	157405
7	codellama/CodeLlama-13b-Instruct-hf (Rozière et al., 2024)	–	llama-2	1	25248
8	meta-llama/Llama-2-13b-hf (Touvron et al., 2023b)	–	llama-2	1	120871
9	meta-llama/Llama-2-7b-hf (Touvron et al., 2023b)	–	llama-2	1	1294737
10	meta-llama/Meta-Llama-3-8B-Instruct (AI@Meta, 2024)	–	llama-3	1	2058011
11	meta-llama/Meta-Llama-3-8B (AI@Meta, 2024)	–	llama-3	1	675850
12	NousResearch/Hermes-2-Pro-Llama-3-8B (“Teknium” et al., 2024b)	–	llama-3	1	26797
13	mistralai/Mistral-7B-Instruct-v0.2 (Jiang et al., 2023)	–	mistral	1	3565248
14	mistralai/Mistral-7B-v0.1 (Jiang et al., 2023)	–	mistral	1	1750089
15	mlabonne/Marcoro14-7B-slerp	–	mistral	1	3792
16	mlabonne/NeuralMonarch-7B	–	mistral	1	13486
17	stabilityai/japanese-stablelm-base-gamma-7b (Jiang et al., 2023)	–	mistral	1	2072
18	beomi/KoRWKV-6B	–	others	1	2127
19	microsoft/Orca-2-13b (Mitra et al., 2023)	–	others	1	13616
20	upstage/SOLAR-10.7B-v1.0 (Kim et al., 2024b)	–	others	1	24478
21	01-ai/Yi-1.5-9B (01. AI et al., 2025)	–	others	1	20252
22	deepseek-ai/DeepSeek-Prover-V1.5-SFT (Xin et al., 2024)	deepseek-ai/DeepSeek-Prover-V1.5-Base	deepseek	2	6459
23	euclaise/falcon_1b_stage1	tiuae/falcon-rw-1b	falcon	2	2119
24	lemon-mint/gemma-ko-7b-instruct-v0.71	google/gemma-1.1-7b-it	gemma	2	2232
25	lemon-mint/gemma-7b-openhermes-v0.80	google/gemma-1.1-7b-it	gemma	2	4867
26	google/gemma-7b-it (Joshi et al., 2017; Mihaylov et al., 2018; Zhao et al., 2018; Rudinger et al., 2018; Bisk et al., 2019; Chollet, 2019; Clark et al., 2019; Talmor et al., 2019; Sap et al., 2019; Zellers et al., 2019; Sakaguchi et al., 2019; Gehman et al., 2020; Chen et al., 2021; Austin et al., 2021; Hendrycks et al., 2021; Dhamala et al., 2021; Cobbe et al., 2021; Lin et al., 2022; Hartvigsen et al., 2022; Parrish et al., 2022; Srivastava et al., 2023; Zhong et al., 2023; Gemini Team et al., 2024)	google/gemma-7b	gemma	2	66776
27	Telugu-LLM-Labs/Indic-gemma-7b-finetuned-sft-Navarasa-2.0	google/gemma-7b	gemma	2	2025
28	lemon-mint/gemma-ko-7b-instruct-v0.62	openchat/openchat-3.5-0106-gemma	gemma	2	7543

ID	Model Name	Base Model Name	Model Type	Generation	DLs
29	rinna/your-7b (Andonian et al., 2021; Touvron et al., 2023b; Zhao et al., 2023; Sawada et al., 2024)	meta-llama/Llama-2-7b-hf	llama-2	2	2512
30	aaditya/Llama3-OpenBioLLM-8B (Singhal et al., 2022; Nori et al., 2023; Singhal et al., 2023; Pal and Sankarasubbu, 2024b,a; Rafailov et al., 2024)	meta-llama/Meta-Llama-3-8B	llama-3	2	9308
31	cognitivecomputations/dolphin-2.9-llama3-8b	meta-llama/Meta-Llama-3-8B	llama-3	2	130977
32	cognitivecomputations/dolphin-2.9.1-llama-3-8b	meta-llama/Meta-Llama-3-8B	llama-3	2	7575
33	DeepMount00/Llama-3-8b-Ita	meta-llama/Meta-Llama-3-8B	llama-3	2	179401
34	dfurman/Llama-3-8B-Orpo-v0.1	meta-llama/Meta-Llama-3-8B	llama-3	2	5146
35	johnsnowlabs/JSL-MedLlama-3-8B-v2.0	meta-llama/Meta-Llama-3-8B	llama-3	2	11813
36	jondurbin/bagel-8b-v1.0	meta-llama/Meta-Llama-3-8B	llama-3	2	7960
37	openchat/openchat-3.6-8b-20240522 (Wang et al., 2024a)	meta-llama/Meta-Llama-3-8B	llama-3	2	10464
38	rinna/llama-3-youko-8b (Andonian et al., 2021; Mitsuda et al., 2024; AI@Meta, 2024; Sawada et al., 2024)	meta-llama/Meta-Llama-3-8B	llama-3	2	1468
39	ruslanmv/Medical-Llama3-8B	meta-llama/Meta-Llama-3-8B	llama-3	2	5457
40	lightblue/suzume-llama-3-8B-multilingual (Devine, 2024)	meta-llama/Meta-Llama-3-8B-Instruct	llama-3	2	16442
41	MaziyarPanahi/Llama-3-8B-Instruct-v0.4	meta-llama/Meta-Llama-3-8B-Instruct	llama-3	2	1407
42	PathFinderKR/Waktaverse-Llama-3-KO-8B-Instruct (AI@Waktaverse, 2024; AI@Meta, 2024)	meta-llama/Meta-Llama-3-8B-Instruct	llama-3	2	2305
43	shenzhi-wang/Llama3-8B-Chinese-Chat (Wang et al., 2024b)	meta-llama/Meta-Llama-3-8B-Instruct	llama-3	2	55718
44	SJ-Donald/llama3-passthrough-chat	meta-llama/Meta-Llama-3-8B-Instruct	llama-3	2	2241
45	swap-uniba/LLaMAAntino-3-ANITA-8B-Inst-DPO-ITA (Basile et al., 2023; AI@Meta, 2024; Polignano et al., 2024)	meta-llama/Meta-Llama-3-8B-Instruct	llama-3	2	5995
46	NousResearch/Hermes-2-Theta-Llama-3-8B ("Teknium" et al., 2024a)	NousResearch/Hermes-2-Pro-Llama-3-8B	llama-3	2	12392
47	vicgalle/Configurable-Hermes-2-Pro-Llama-3-8B (Gallego, 2024)	NousResearch/Hermes-2-Pro-Llama-3-8B	llama-3	2	10273
48	abacusai/bigstral-12b-32k	mistralai/Mistral-7B-Instruct-v0.2	mistral	2	5216
49	Mihaiii/Metis-0.3	mistralai/Mistral-7B-Instruct-v0.2	mistral	2	1279
50	alignment-handbook/zephyr-7b-sft-full	mistralai/Mistral-7B-v0.1	mistral	2	11605
51	cognitivecomputations/dolphin-2.2.1-mistral-7b	mistralai/Mistral-7B-v0.1	mistral	2	7292
52	cypienai/cymist-2-v02-SFT (Lacoste et al., 2019)	mistralai/Mistral-7B-v0.1	mistral	2	2717
53	HuggingFaceH4/mistral-7b-sft-beta	mistralai/Mistral-7B-v0.1	mistral	2	7408
54	HuggingFaceH4/zephyr-7b-alpha (Ding et al., 2023; Tunstall et al., 2023; Cui et al., 2024; Rafailov et al., 2024)	mistralai/Mistral-7B-v0.1	mistral	2	12911
55	HuggingFaceH4/zephyr-7b-beta (Ding et al., 2023; Tunstall et al., 2023; Cui et al., 2024; Rafailov et al., 2024)	mistralai/Mistral-7B-v0.1	mistral	2	294019
56	ibm/merlinit-7b (Sudalairaj et al., 2024)	mistralai/Mistral-7B-v0.1	mistral	2	11156
57	INSAIT-Institute/BgGPT-7B-Instruct-v0.2	mistralai/Mistral-7B-v0.1	mistral	2	3265
58	Intel/neural-chat-7b-v3-1 (Mukherjee et al., 2023)	mistralai/Mistral-7B-v0.1	mistral	2	3976
59	kaist-ai/mistral-orpo-capybara-7k (Hong et al., 2024)	mistralai/Mistral-7B-v0.1	mistral	2	4821
60	Locutusque/Hercules-2.5-Mistral-7B	mistralai/Mistral-7B-v0.1	mistral	2	1953
61	mistralai/Mistral-7B-Instruct-v0.1 (Jiang et al., 2023)	mistralai/Mistral-7B-v0.1	mistral	2	1370245
62	NousResearch/Hermes-2-Pro-Mistral-7B ("interstellarninja" et al., 2024)	mistralai/Mistral-7B-v0.1	mistral	2	14586
63	NousResearch/Nous-Hermes-2-Mistral-7B-DPO ("Teknium" et al., 2024c)	mistralai/Mistral-7B-v0.1	mistral	2	8725
64	openchat/openchat-3.5-0106 (Wang et al., 2024a; OpenAI et al., 2024)	mistralai/Mistral-7B-v0.1	mistral	2	26858
65	openchat/openchat-3.5-1210 (Wang et al., 2024a; OpenAI et al., 2024)	mistralai/Mistral-7B-v0.1	mistral	2	2123
66	statking/zephyr-7b-sft-full-orpo	mistralai/Mistral-7B-v0.1	mistral	2	2278
67	teknium/OpenHermes-2.5-Mistral-7B	mistralai/Mistral-7B-v0.1	mistral	2	100997
68	mlabonne/NeuralMarco14-7B	mistralai/Marco14-7B-slerp	mistral	2	2015
69	mlabonne/AlphaMonarch-7B	mlabonne/NeuralMonarch-7B	mistral	2	12804
70	augmnt/shisa-gamma-7b-v1	stabilityai/japanese-stablelm-base-gamma-7b	mistral	2	151426
71	beomi/KoAlpaca-KoRWKV-6B	beomi/KoRWKV-6B	others	2	2288
72	Nexusflow/NexusRaven-V2-13B (Nexusflow.ai team, 2023; Rozière et al., 2024)	codellama/CodeLlama-13b-Instruct-hf	others	2	3966
73	haoranxu/ALMA-13B-Pretrain (Xu et al., 2024a,b)	meta-llama/Llama-2-13b-hf	others	2	5510
74	ruslanmv/ai-medical-model-32bit	meta-llama/Meta-Llama-3-8B-Instruct	others	2	2810
75	Locutusque/Orca-2-13b-SFT-v4	microsoft/Orca-2-13b	others	2	2345
76	Locutusque/Orca-2-13b-SFT-v6	microsoft/Orca-2-13b	others	2	2319
77	Locutusque/Orca-2-13b-SFT_v5	microsoft/Orca-2-13b	others	2	2191
78	mwitiderrick/open_llama_3b_code_instruct_0.1	openlm-research/open_llama_3b	others	2	1252
79	NousResearch/Nous-Hermes-2-SOLAR-10.7B	upstage/SOLAR-10.7B-v1.0	others	2	9918
80	upstage/SOLAR-10.7B-Instruct-v1.0 (Kim et al., 2024b,a)	upstage/SOLAR-10.7B-v1.0	others	2	67725
81	cognitivecomputations/dolphin-2.9.1-yi-1.5-9b	01-ai/Yi-1.5-9B	others	2	4880
82	deepseek-ai/DeepSeek-Prover-V1.5-RL (Xin et al., 2024)	deepseek-ai/DeepSeek-Prover-V1.5-SFT	deepseek	3	12223
83	euclaise/falcon_1b_stage2	euclaise/falcon_1b_stage1	falcon	3	4016
84	MaziyarPanahi/Llama-3-8B-Instruct-v0.8	MaziyarPanahi/Llama-3-8B-Instruct-v0.4	llama-3	3	7281
85	argilla/notus-7b-v1	alignment-handbook/zephyr-7b-sft-full	mistral	3	7660
86	Intel/neural-chat-7b-v3-3 (Yu et al., 2024)	Intel/neural-chat-7b-v3-1	mistral	3	166226
87	MaziyarPanahi/Llama-3-8B-Instruct-v0.9	MaziyarPanahi/Llama-3-8B-Instruct-v0.8	llama-3	4	6241

Table 7: List of 59 models in the experiments for layer-wise models. “ID” denotes the index sorted in descending order of downloads; “Model Name” denotes the name of the model; “Model Type” denotes the model classification defined in Oyama et al. (2025); “Layers” denotes the number of layers in the model; “DLs” denotes the total number of downloads.

ID	Model Name	Model Type	Layers	DLs
1	mistralai/Mistral-7B-Instruct-v0.2 (Jiang et al., 2023)	mistral	32	3565248
2	meta-llama/Meta-Llama-3-8B-Instruct (AI@Meta, 2024)	llama-3	32	2058011
3	mistralai/Mistral-7B-v0.1 (Jiang et al., 2023)	mistral	32	1750089
4	mistralai/Mistral-7B-v0.3	mistral	32	1443065
5	meta-llama/Llama-2-7b-chat-hf (Touvron et al., 2023b)	llama-2	32	1402244
6	mistralai/Mistral-7B-Instruct-v0.1 (Jiang et al., 2023)	mistral	32	1370245
7	meta-llama/Llama-2-7b-hf (Touvron et al., 2023b)	llama-2	32	1294737
8	TinyLlama/TinyLlama-1.1B-Chat-v1.0	others	22	1078500
9	TinyLlama/TinyLlama-1.1B-intermediate-step-1431k-3T	others	22	798206
10	meta-llama/Meta-Llama-3-8B (AI@Meta, 2024)	llama-3	32	675850
11	OpenAssistant/oasst-sft-4-pythia-12b-epoch-3.5	gpt_neox	36	458718
12	bigcode/starcoder2-3b (Beltagy et al., 2020; Dao et al., 2022; Bavarian et al., 2022; Ainslie et al., 2023; Lozhkov et al., 2024)	others	30	445316
13	lmsys/vicuna-7b-v1.5 (Touvron et al., 2023b; Zheng et al., 2023)	llama-2	32	368410
14	HuggingFaceH4/zephyr-7b-beta (Ding et al., 2023; Tunstall et al., 2023; Cui et al., 2024; Rafailov et al., 2024)	mistral	32	294019
15	meta-llama/Llama-2-13b-chat-hf (Touvron et al., 2023b)	llama-2	40	266090
16	google/gemma-2b (Joshi et al., 2017; Mihaylov et al., 2018; Zhao et al., 2018; Rudinger et al., 2018; Bisk et al., 2019; Chollet, 2019; Clark et al., 2019; Talmor et al., 2019; Sap et al., 2019; Zellers et al., 2019; Sakaguchi et al., 2019; Gehman et al., 2020; Chen et al., 2021; Austin et al., 2021; Hendrycks et al., 2021; Dhamala et al., 2021; Cobbe et al., 2021; Lin et al., 2022; Hartvigsen et al., 2022; Parrish et al., 2022; Srivastava et al., 2023; Zhong et al., 2023; Gemini Team et al., 2024)	gemma	18	256798
17	EleutherAI/gpt-neo-1.3B (Gao et al., 2020; Black et al., 2021)	others	24	243332
18	EleutherAI/gpt-j-6b (Gao et al., 2020; Wang and Komatsuzaki, 2021; Wang, 2021; Su et al., 2023)	gptj	28	241435
19	microsoft/phi-2	others	32	237268
20	EleutherAI/gpt-neo-2.7B (Gao et al., 2020; Black et al., 2021)	others	32	205503
21	huggyllama/llama-7b	llama-1	32	192383
22	tiuae/falcon-7b-instruct (Shazeer, 2019; Brown et al., 2020; Dao et al., 2022; Su et al., 2023; Almazrouei et al., 2023; Penedo et al., 2023)	falcon	32	179952
23	DeepMount00/Llama-3-8b-Ita	llama-3	32	179401
24	Intel/neural-chat-7b-v3-3 (Yu et al., 2024)	mistral	32	166226
25	openlm-research/open_llama_3b (Together Computer, 2023; Touvron et al., 2023a; Geng and Liu, 2023)	llama-1	26	157405
26	augmnt/shisa-gamma-7b-v1	mistral	32	151426
27	facebook/opt-1.3b (Brown et al., 2020; Zhang et al., 2022)	opt	24	139758
28	Qwen/Qwen1.5-1.8B (Bai et al., 2023)	others	24	137256
29	codellama/CodeLlama-7b-Instruct-hf (Rozière et al., 2024)	llama-2	32	133523
30	cognitivecomputations/dolphin-2.9-llama3-8b	llama-3	32	130977
31	Qwen/Qwen1.5-7B (Bai et al., 2023)	others	32	122768
32	meta-llama/Llama-2-13b-hf (Touvron et al., 2023b)	llama-2	40	120871
33	microsoft/phi-1.5 (Li et al., 2023)	others	24	112476
34	NousResearch/Meta-Llama-3-8B-Instruct (AI@Meta, 2024)	llama-3	32	104388
35	tiuae/falcon-7b (Shazeer, 2019; Brown et al., 2020; Gao et al., 2020; Dao et al., 2022; Su et al., 2023; Almazrouei et al., 2023; Penedo et al., 2023)	falcon	32	104010
36	google/gemma-2b-it (Joshi et al., 2017; Mihaylov et al., 2018; Zhao et al., 2018; Rudinger et al., 2018; Bisk et al., 2019; Chollet, 2019; Clark et al., 2019; Talmor et al., 2019; Sap et al., 2019; Zellers et al., 2019; Sakaguchi et al., 2019; Gehman et al., 2020; Chen et al., 2021; Austin et al., 2021; Hendrycks et al., 2021; Dhamala et al., 2021; Cobbe et al., 2021; Lin et al., 2022; Hartvigsen et al., 2022; Parrish et al., 2022; Srivastava et al., 2023; Zhong et al., 2023; Gemini Team et al., 2024)	gemma	18	103851
37	teknium/OpenHermes-2.5-Mistral-7B	mistral	32	100997
38	mosaicml/mpt-7b-chat (Henry et al., 2020; Press et al., 2022; Dao et al., 2022; MosaicML NLP Team, 2023)	others	32	88069
39	Qwen/CodeQwen1.5-7B-Chat (Bai et al., 2023)	others	32	77169
40	GritLM/GritLM-7B (Muennighoff et al., 2025)	mistral	32	72991
41	google/gemma-7b (Joshi et al., 2017; Mihaylov et al., 2018; Zhao et al., 2018; Rudinger et al., 2018; Bisk et al., 2019; Chollet, 2019; Clark et al., 2019; Talmor et al., 2019; Sap et al., 2019; Zellers et al., 2019; Sakaguchi et al., 2019; Gehman et al., 2020; Chen et al., 2021; Austin et al., 2021; Hendrycks et al., 2021; Dhamala et al., 2021; Cobbe et al., 2021; Lin et al., 2022; Hartvigsen et al., 2022; Parrish et al., 2022; Srivastava et al., 2023; Zhong et al., 2023; Dettmers et al., 2023; Gemini Team et al., 2024)	gemma	28	72047
42	upstage/SOLAR-10.7B-Instruct-v1.0 (Kim et al., 2024b,a)	others	48	67725
43	google/gemma-7b-it (Joshi et al., 2017; Mihaylov et al., 2018; Zhao et al., 2018; Rudinger et al., 2018; Bisk et al., 2019; Chollet, 2019; Clark et al., 2019; Talmor et al., 2019; Sap et al., 2019; Zellers et al., 2019; Sakaguchi et al., 2019; Gehman et al., 2020; Chen et al., 2021; Austin et al., 2021; Hendrycks et al., 2021; Dhamala et al., 2021; Cobbe et al., 2021; Lin et al., 2022; Hartvigsen et al., 2022; Parrish et al., 2022; Srivastava et al., 2023; Zhong et al., 2023; Gemini Team et al., 2024)	gemma	28	66776
44	codellama/CodeLlama-7b-hf (Rozière et al., 2024)	llama-2	32	66040
45	facebook/opt-2.7b (Brown et al., 2020; Zhang et al., 2022)	opt	32	61450
46	shenzhi-wang/Llama3-8B-Chinese-Chat (Wang et al., 2024b)	llama-3	32	55718
47	VAGOSolutions/Llama-3-SauerkrautLM-8b-Instruct	llama-3	32	55400
48	lmsys/vicuna-13b-v1.5 (Touvron et al., 2023b; Zheng et al., 2023)	llama-2	40	48653
49	Qwen/Qwen2-1.5B (Yang et al., 2024)	others	28	46510
50	openlm-research/open_llama_7b (Together Computer, 2023; Touvron et al., 2023a; Geng and Liu, 2023)	llama-1	32	44968
51	LinkSoul/Chinese-Llama-2-7b	llama-2	32	40799
52	mistral-community/Mistral-7B-v0.2	mistral	32	30074
53	NousResearch/Hermes-2-Pro-Llama-3-8B ("Teknium" et al., 2024b)	llama-3	32	26797
54	lightblue/suzume-llama-3-8B-multilingual (Devine, 2024)	llama-3	32	16442
55	abacusai/Llama-3-Smaug-8B (Pal et al., 2024)	llama-3	32	12873
56	NousResearch/Nous-Hermes-llama-2-7b	llama-2	32	12019
57	togethercomputer/LLaMa-2-7B-32K	llama-2	32	8884
58	elyza/ELYZA-japanese-Llama-2-7b-instruct (Touvron et al., 2023b; Sasaki et al., 2023)	llama-2	32	6296
59	togethercomputer/Llama-2-7B-32K-Instruct (Liu et al., 2023)	llama-2	32	5596